

# Electromagnetic-Field-Based Circuit Theory and Charge-Flux-Flow Diagrams

Yongliang Wang <sup>a,b\*</sup> *Member, IEEE*

<sup>a</sup> *Shanghai Institute of Microsystem and Information Technology (SIMIT), Chinese Academy of Sciences (CAS), Shanghai 200050, China*

<sup>b</sup> *CAS Center for Excellence in Superconducting Electronics, Shanghai 200050, China*

\*Corresponding author. Tel.: +86 02162511070; Fax: +86 02162127493.

E-mail address: [wangyl@mail.sim.ac.cn](mailto:wangyl@mail.sim.ac.cn); ORCID: [Yong-Liang Wang \(0000-0001-7263-9493\)](https://orcid.org/0000-0001-7263-9493)

Major references: <https://doi.org/10.1109/TASC.2022.3162913>.

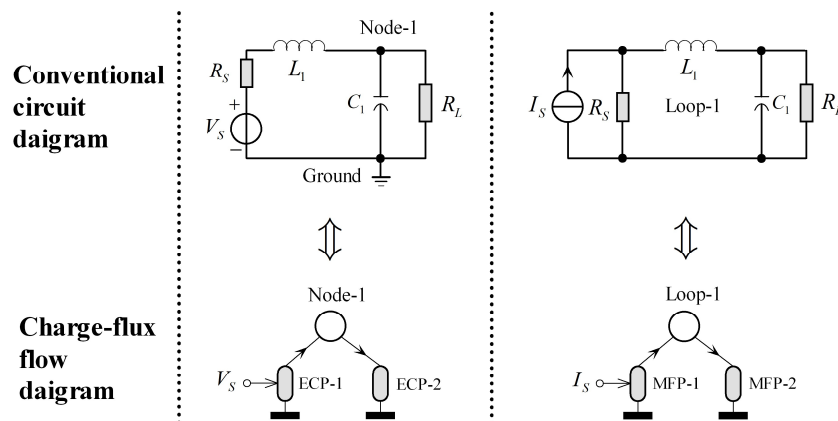
<https://doi.org/10.1109/TASC.2023.3290199>.

<https://doi.org/10.48550/arXiv.2308.01693>.

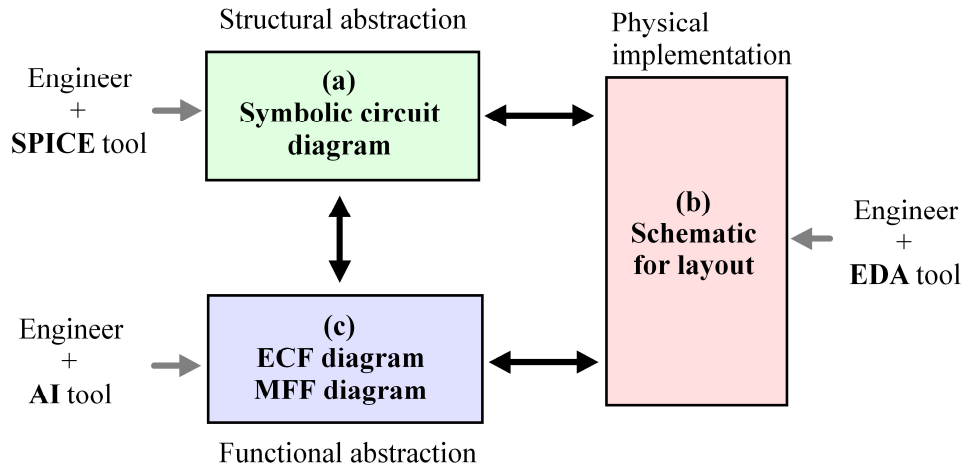
## Abstract

The conventional circuit diagrams and graph-based circuit theory are used for the phase-independent circuits such as resistor-inductor-capacitor (RLC) circuits and semiconductor transistor circuits, rather than for the phase-dependent circuits such as Josephson junction circuits and quantum-phase-slip (QPS) junction circuits. To unify the analyses for both phase-independent and phase-dependent electric circuits, we develop an electromagnetic-field-based circuit theory and invent the electric-charge-flow (ECF) and the magnetic-flux-flow (MFF) diagrams to derive the general circuit equations and visualizes the dynamics of circuit devices for all kinds of electric circuits. ECF and MFF diagrams enable electric circuits to be described like the molecules composed of two kinds of atoms; they are new languages for circuit design and analysis, promising for machine-learning.

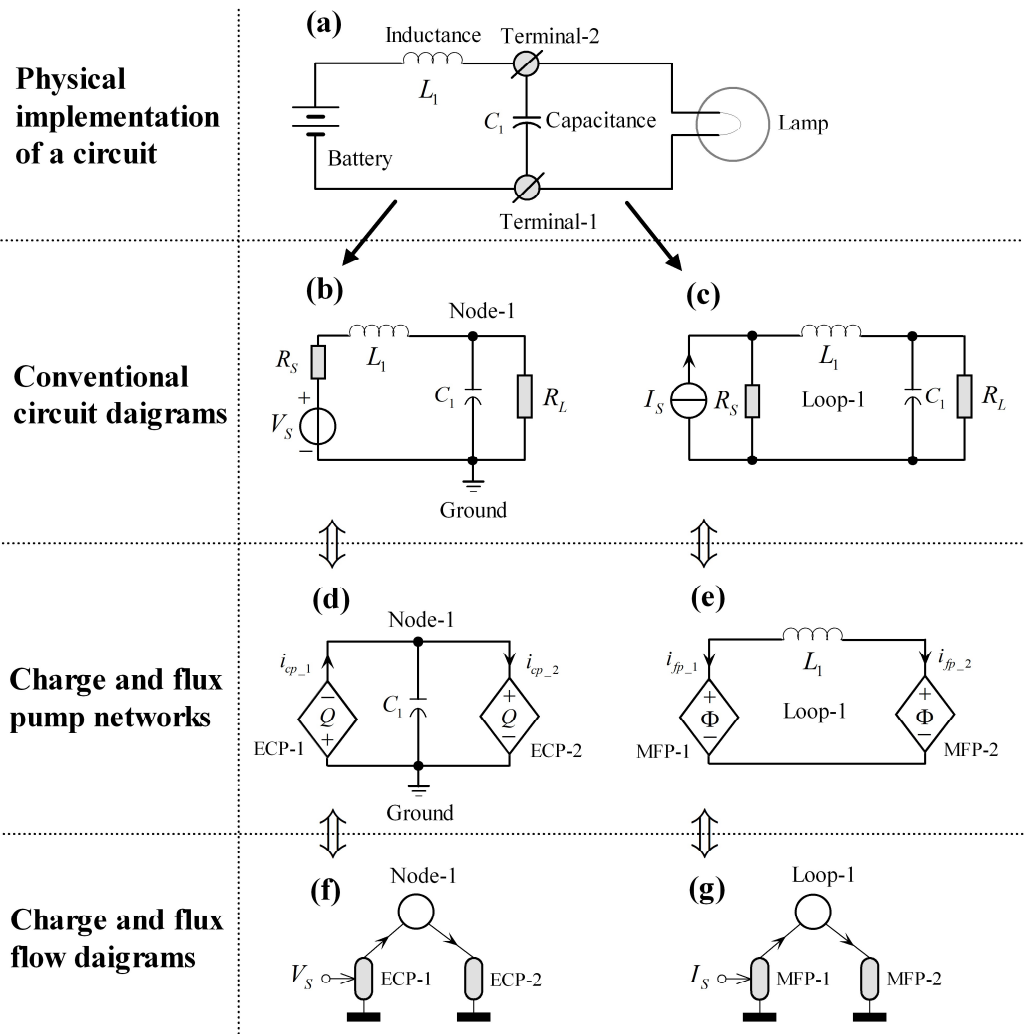
*Keywords:* charge-based circuit theory, flux-based circuit theory, ECF diagram, MFF diagram, Josephson junction circuit, QPS junction circuit, AI-aided circuit design.



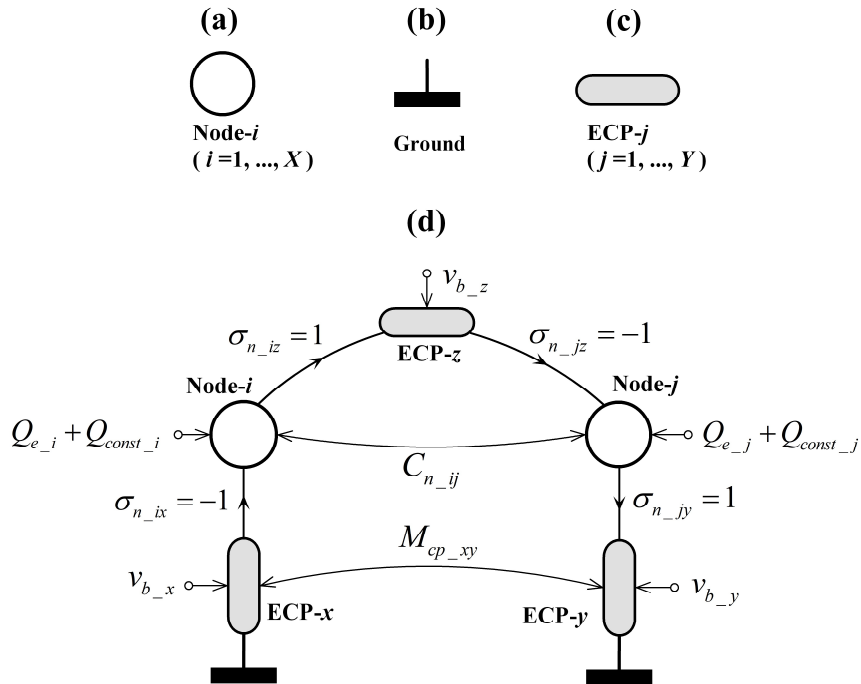
## Diagrams for Circuit Design



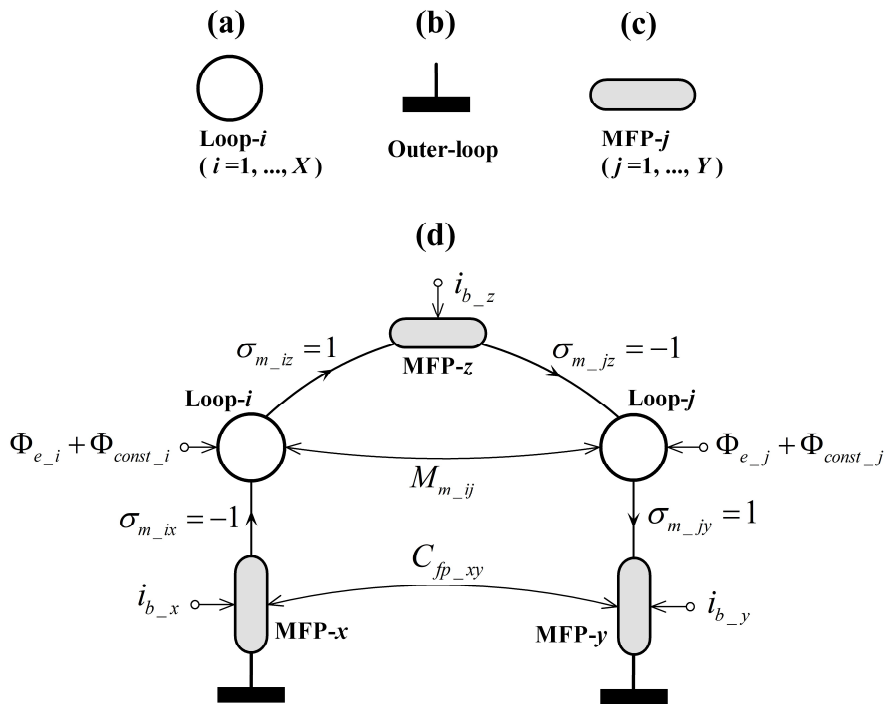
## Example of Circuit Diagrams



### Electric-charge-flow (ECF) Diagram



### Magnetic-flux-flow (MFF) Diagram



# 1. Introduction

Electric circuits are charge-flow network implemented by interconnecting electrical devices with wires, where the charge carriers are driven by electric and magnetic fields; they are used to transmit electric energy and signals [1], for both analog and digital applications. Charges in electric circuits are driven by the electric and magnetic fields; their working principles are described by the Maxwell's equations, while the circuit analysis is still based on the graph-theory and the Kirchhoff's laws [2], which is firstly developed by Prof. Ernst Guillemin in 1930s [3]. For physical implementation, an electric circuit will be firstly drawn as a schematic to describe its physical structure, and for circuit analyses, it will be turned into a symbolic circuit diagram, The schematic is supported by electronic-design-automation (EDA) tools [4] for layout or the printed-circuit-board (PCB) design. The symbolic circuit diagram is the structural abstraction of the schematic; it uses Kirchhoff's laws to model the electromagnetic principles in circuits, and can be processed by the SPICE (simulation program with integrated circuit emphasis) tools for numerical simulations [5-9].

In the coming era of artificial-intelligence (AI), AI-aided tools for integrated circuits design are on the quick developing [10-12]. Do we still have to use the conventional schematics or symbolic circuit diagrams to train AI tools? Are there new circuit diagrams that are more suitable for the AI tools? In this article, we introduce an electromagnetic-field-based circuit theory and the charge-flux-flow diagrams to upgrade the circuit analysis methodologies for AI tools. The electric-charge flow (ECF) and magnetic-flux flow (MFF) diagrams are the functional abstractions of electric circuits [13, 14]. Three types of circuit diagrams are compared in Fig. 1.

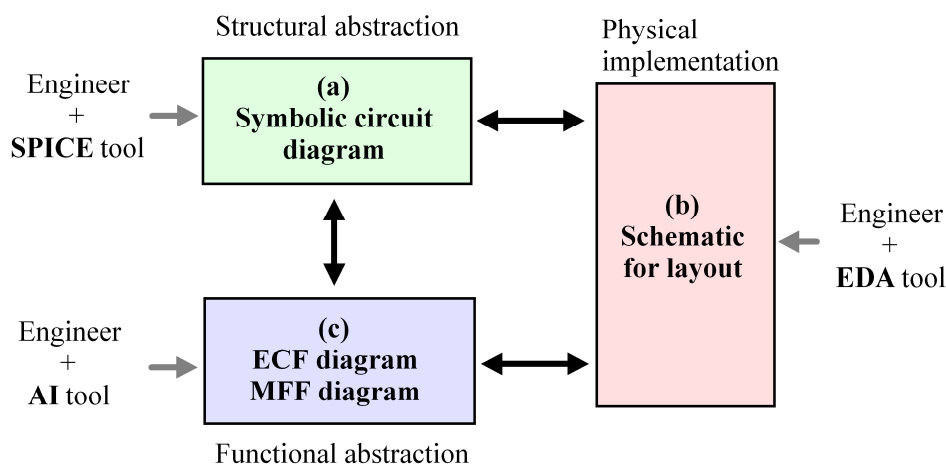


Fig. 1. Three kinds of circuit diagrams: (a) symbolic circuit diagrams used for circuit analyses, supported by SPICE tools; (b) the schematics for physical implementation, supported by EDA tools; (c) the electric-charge-flow (ECF) diagrams and magnetic-flux-flow diagram (MFF) diagrams for functional abstraction of electric circuits; they can be used to train artificial intelligence (AI) tools.

## 2. Evolution of circuit diagrams

### A. An overview

The evolution of circuit diagrams is illustrated in Fig. 2, where a simple electric circuit and its circuit diagrams for different levels of abstraction are exhibited.

1) **Schematic is the wiring diagram for physical implementation:** Fig. 2(a) is the schematic of the example circuit, which is implemented by connecting a battery and a lamp with wires to two terminals.

2) **Symbolic circuit diagram is the graph-theory-based model for deriving circuit equations:** Symbolic circuit diagrams are the equivalent circuits composed of basic resistor-inductor-capacitor (RLC) elements, as shown in Fig. 2(b) and (c). The circuit is further modeled as an electric-charge pump (ECP) network for charge-based analysis, as shown in Fig. 2(d), and as a magnetic-flux pump (MFP) network for flux-based analysis, as shown in Fig. 2(e).

3) **Electric-charge flow (ECF) diagram is the interaction diagram of ECP network, and Magnetic-flux flow (MFF) diagram is the interaction diagram of MFP network:** ECF diagram is composed of ECPs and nodes, and MFF diagram is consisted of MFPs and loops, as shown in Fig. 2(f) and (g).

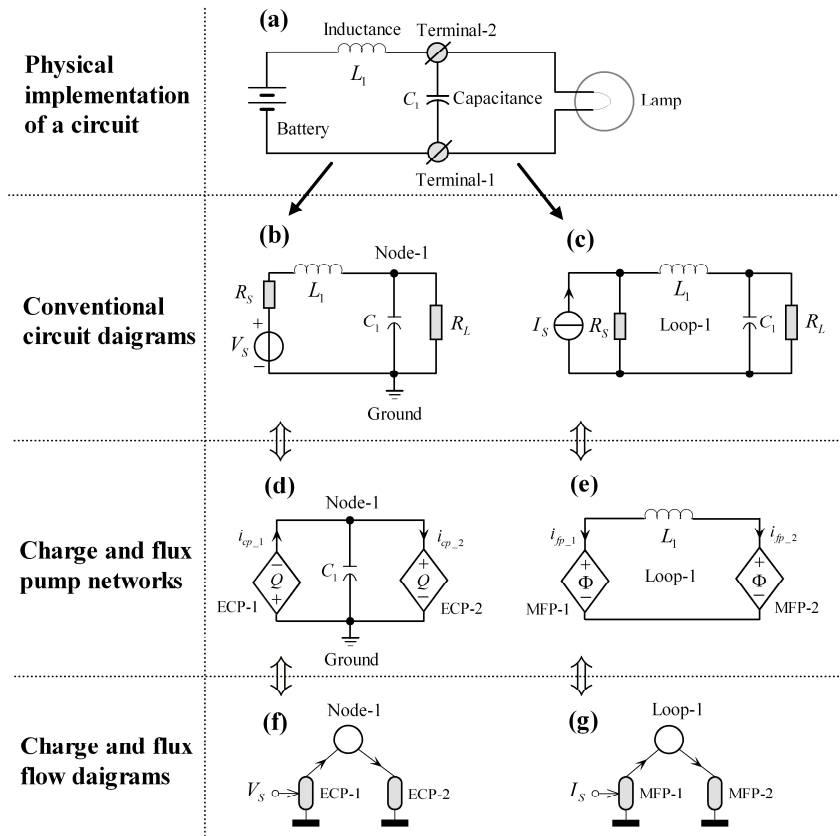


Fig. 2. Diagrams for an example circuit; (a) a schematic; (b) circuit diagram with Thevenin's equivalent; (c) circuit diagram with Norton's equivalent; (d) charge-pump network; (e) flux-pump network; (f) ECF diagram; (g) MFF diagram.

## B. Schematic for physical implementation

**Circuit schematics are wiring diagrams drawn according to the what-you-see-is-what-you-get (WYSIWYG) principle;** they consist of two kinds of objects:

1) Circuit components. A block with pins represents a component in schematics; pins of components are connected to nodes with wires.

2) Wires. Wires are conductors that connect component pins to nodes.

Schematics emphasize the connections between components, they are drawn for circuit layout or printed-circuit-board (PCB) design with electronic-design-automation (EDA) tools. to further derive circuit equations for circuit analyses, a schematic will be redrawn with a symbolic circuit diagram.

## C. Symbolic circuit diagram for deriving circuit equations

**Symbolic circuit diagrams are equivalent circuits of schematics for circuit analyses;** they are drawn with the equivalent circuit of devices.

1) The functions of components in schematics are implemented with their equivalent circuits. Those equivalent circuits are described by the SPICE models in SPICE tools [5, 6, 15, 16]; they are consisted of basic elements, such as resistor (R), inductor (L), capacitor (C), PN junction, voltage and current sources [17-19].

2) The resistance, capacitance, and inductance effects of wires are implemented with RLC elements. For example, the resistance is implemented with a resistor inserted in wire; the electric field couplings between wires are implemented with the capacitors connected between nodes; the magnetic field couplings between wires are implemented with inductors coupled through mutual inductances.

For instance, Fig. 2(b) and (c) are two symbolic circuit diagrams of the example circuit. In Fig. 2(b), the battery is modeled with the Thevenin's equivalent circuit, and in Fig. 2(c) the battery is modeled with the Norton's equivalent.

Symbolic circuit diagrams are composed of nodes and branches; branches are implemented with basic two-terminal circuit elements. We can extract nodes, branches, and faces from diagrams and derive the circuit equations, based on the graph theory. In a given graph, assuming that the number of branches is  $b$ , the number of nodes is  $n-1$  (except the datum node), and the number of independent loops is  $f$ , each branch is defined by its branch current  $i_{br}$  and branch voltage  $v_{br}$ , and the number of variables is  $2b$ ; the full-rank equations of  $i_{br}$  and  $v_{br}$  are set up by combining

1) **the VCR functions for branches,**

2) **the equations of  $i_{br}$  at nodes,** using Kirchhoff's current law (KCL),

3) **the equations of  $v_{br}$  in loops,** using Kirchhoff's voltage law (KVL).

Those circuit equations are automatically derived in SPICE tools by using the general modified-nodal-analysis (MNA) method [20].

The symbolic circuit diagrams, are the mathematic model, rather than the physical model of electric circuits; the KCL and KVL are mathematic constraints, instead of the principles of electromagnetic fields.

1) The KCL states that the algebraic sum of all the  $i_{br}$  flowing in and out of a node is null [21], which assumes that **there are no extra charges stored at nodes.**

2) The KVL states that the algebraic sum of all the  $v_{br}$  inserted in a loop is null [21], which assumes that **there are no extra fluxes coupled in loops**.

However, in practical circuits, node voltages will attract charges gathering at nodes, and branch currents will induce magnetic fluxes in loops. To meet KCL and KVL, the circuit diagram for practical electric circuits will be amended using capacitors, inductors, mutual inductances:

1) **Capacitors** are connected between nodes to store the charges aroused by node voltages.

2) **Inductors** are inserted in branches to store the fluxes induced by branch currents.

3) **Mutual inductances** between inductors are defined to the magnetic couplings between branches.

The graph-theory-based circuit diagrams is disadvantageous for the circuits with mutual inductances. A circuit diagram will be a complex N-port network that is difficult to analysis, if it includes all the mutual inductances between branches.

#### D. Challenges of conventional circuit theory

The conventional circuit theory based on the symbolic circuit diagrams, has achieved great success in the design and analysis of **phase-independent** circuits such as normal resistor-inductor-capacitor (RLC) circuits and semiconductor electronic circuits. It meets challenges in the analyses of the **phase-dependent** circuits such as Josephson junction circuits [22-26] and quantum-phase-slip (QPS) junction circuits [27-32]. Here, the phase refers to the variables that are associated with the charges stored at nodes, the fluxes coupled in loops, and the charges or fluxes flowing through circuit elements. The differences between phase-independent and phase-dependent circuits are compared in Table 1. The disadvantages of the conventional circuit theory are:

1) **The VCRs are used to define phase-independent circuit elements** such as the RLC elements and semiconductor transistors. Josephson junctions are defined with flux-current-relations (FCRs), and QPS junctions are described with charge-voltage-relations (QVRs).

2) **The KCL and KVL are the laws for phase-independent circuits**. The charge-quantization law (CQL), instead of KCL, is used in the analysis of QPS-junction circuits, and the flux-quantization law (FQL), instead of the KVL, is used in the analysis of Josephson-junction circuits.

Table 1. Features of phase-independent and phase-dependent circuits

	Phase-independent circuits	Phase-dependent circuits
Definition of Elements	VCR	FCR for Josephson junctions; QVR for QPS junctions
Circuit law at nodes	KCL	CQL for QPS circuits
Circuit law at loops	KVL	FQL for Josephson circuits

Symbolic circuit diagrams are the equivalent mathematic models of practical electric circuits, where, capacitors between nodes, inductors in branches, and the mutual inductances between branches, are the mathematic approaches to describe the effects

of electric and magnetic fields. By redefining the voltages with phase-dependent variables, the voltage-based MNA method can be upgraded to the so-called phased-based MNA method [16, 33], nevertheless, two problems remain unsolved.

1) **Conventional circuit diagrams will conceal the charge quanta at nodes**, in modeling QPS junction circuits; they divide and assign the quantized charges stored at nodes to the capacitors connected between nodes.

2) **Conventional circuit diagrams will conceal the flux quanta in loops**, in modeling Josephson junction circuits; they divide and assign the quantized fluxes coupled in loops to the inductors inserted in the loops, and the inductors are coupled with mutual inductances.

### *E. Electromagnetic-flux-distribution models*

To unify the design and analysis of phase-independent and phase-dependent circuits, we develop an electromagnetic-field-based circuit theory, based on the electromagnetic-flux distribution models [21]. In this theory, an electric circuit can be modeled as either an ECP network for charge-based analysis, or an MFP network for flux-based analysis. Fig. 2(d) shows the ECP network of the example circuit, and Fig. 2(e) depicts the MFP network for the example circuit:

1) **ECP network is composed of electric-charge containers (ECCs) and electric-charge pumps (ECPs)**, where ECPs pump charges in and out of ECCs, and ECCs store charges and generate nodal voltages to drive ECPs. The ECPs are the components of non-capacitance elements connected in serial; they are defined with QVR for both phase-independent and phase-dependent circuit elements. The ECCs are the nodes that store charges through capacitors connected between nodes. **The charge-conservation law (CCL) of ECCs unifies the KCL and CQL for both phase-independent and phase-dependent circuits.**

2) **The MFP network is composed of magnetic-flux containers (MFCs) and magnetic-flux pumps (MFPs)**, where MFPs pump magnetic fluxes in and out of MFCs, while MFCs preserve fluxes and generate loop currents to drive MFPs. The MFPs are the components of non-inductance elements connected in parallel; they are defined with FCR for both phase-independent and phase-dependent circuit elements. MFCs are the loops that preserve fluxes with self-inductances of loops and mutual-inductances between loops. **The flux-conservation law (FCL) of MFCs unifies the KVL and FQL for both phase-independent and phase-dependent circuits.**

The features of ECP and MFP networks are summarized in Table 2. It is shown that one circuit can be modeled as an ECP network or an MFP network, like a coin has two sides. This is what we call the charge-flux duality in one circuit [21], similar with the waver-particle duality of light.

To be noticed that **ECP and MFP networks are composed of two kinds of objects more than just two kinds of circuit elements**. The ECCs are more than just the vertexes in the graph shown in Fig. 2(d); they are objects that store charges with capacitances; the MFCs are more than just the loops of the graph shown in Fig. 2(e); they are objects that store fluxes with inductances. **Conventional circuit diagrams are**



**not capable to depict the interactions between objects, for ECP networks and MFP networks.**

Table 2. Features of charge-distribution and flux-distribution networks

	ECP network	MFP network
Energy carrier	Charge	Flux
Field container	ECC	MFC
Field regulator	ECP	MFP
Circuit laws	CCL and energy conservation law	FCL and energy conservation law
Diagram	ECF diagram	MFF diagram

### F. Interaction Diagrams

**Electric-charge-flow diagram (ECF) [14] is the interaction diagram of ECP network, and magnetic-flux-flow (MFF) diagram [13] is the interaction of MFP network.** The ECF and MFF diagrams for the example circuit are illustrated in Fig. 2(f) and (g). ECF and MFF diagrams are the graphic languages that implement the complete descriptions for any given electric circuit; they are promising to be used to train artificial intelligence (AI) for integrated circuit design. Details of the electromagnetic-field-based circuit theory and the flux-charge-flow diagrams are described in the following sections:

- 1) In section 3, we will derive **two dynamic models** of electric circuits, based on the Maxwell's equations of electromagnetic fields.
- 2) In section 4, we will introduce the **flux-charge duality** of electric circuits, and the concepts of charge-based and flux-based analyses.
- 3) In section 5, the **charge-based circuit theory** and ECF diagrams are introduced.
- 4) In section 6, the **flux-based circuit theory** and MFF diagrams are introduced.
- 5) In section 7, the features and applications of the electromagnetic-field-based circuit theory are discussed and summarized.

### 3. Electromagnetics in electric circuits

#### A. Components of electromagnetic fields

**Charges are the carriers of the fluids circulating inside electric circuits;** the conservation law for charge fluids is

$$\nabla \cdot \bar{J} + \frac{\partial \rho}{\partial t} = 0 \quad (1)$$

where  $\rho$  is the density of charges,  $J$  is the density of charge-flow.

In the Maxwell's equations [34], the electric fields that force the charge carriers flowing through circuit devices, is consisted of **three components**:

$$\bar{E} = \bar{E}_{Col} + \bar{E}_{Far} + \bar{E}_{Max} \Rightarrow \begin{cases} \bar{E}_{Col} = -\nabla v, \nabla \cdot \bar{E}_{Col} = \frac{\rho}{\epsilon} \\ \bar{E}_{Far} = -\frac{\partial \bar{A}_{Amp}}{\partial t} \\ \bar{E}_{Max} = -\frac{\partial \bar{A}_{Max}}{\partial t} \end{cases} \quad (2)$$

$$\text{where, } \begin{cases} \nabla \times \bar{A}_{Amp} = \bar{B}_{Amp} \\ \nabla \cdot \bar{A}_{Amp} = 0 \\ \nabla \times \bar{A}_{Max} = \bar{B}_{Max} \\ \nabla \cdot \bar{A}_{Max} = 0 \end{cases} \text{ and } \begin{cases} \nabla \times \bar{B}_{Amp} = \mu \left( \bar{J} + \epsilon \frac{\partial \bar{E}_{Col}}{\partial t} \right) \\ \nabla \cdot \bar{B}_{Amp} = 0 \\ \nabla \times \bar{B}_{Max} = \mu \epsilon \frac{\partial (\bar{E}_{Far} + \bar{E}_{Max})}{\partial t} \\ \nabla \cdot \bar{B}_{Max} = 0 \end{cases}$$

- 1) The  $E_{Col}$  is the **Coulomb's field** set up by charges;
- 2) The  $E_{Far}$  is the **Faraday's field** induced by magnetic field;
- 3) The  $E_{Max}$  is the **Maxwell's field** induced by electric field.

Three electric field components are expressed by **three potentials**:

- 1) The first one is the **Coulomb's scalar potential**  $v$ ; it is set up by charges, and is defined by the Poisson's equation as

$$\left. \begin{cases} \nabla \cdot \bar{E}_{Col} = \frac{\rho}{\epsilon} \\ \bar{E}_{Col} = -\nabla v \end{cases} \right\} \Rightarrow \nabla^2 v = -\frac{\rho}{\epsilon} \quad (3)$$

- 2) The second one is the **Ampere's vector potential**  $A_{Amp}$ ;  $A_{Amp}$  is generated by  $J$  and the variation of  $E_{Col}$ ; its mathematic expressions are derived as

$$\left. \begin{cases} \nabla \times \bar{B}_{Amp} = \mu \left( \bar{J} + \epsilon \frac{\partial \bar{E}_{Col}}{\partial t} \right) \\ \nabla \cdot \bar{E}_{Col} = \frac{\rho}{\epsilon} \\ \nabla \cdot \bar{J} + \frac{\partial \rho}{\partial t} = 0 \end{cases} \right\} \Rightarrow \begin{cases} \nabla^2 \bar{A}_{Amp} = -\mu (\bar{J} + \bar{J}_{Col}) \\ \nabla \cdot (\bar{J} + \bar{J}_{Col}) = 0 \\ \text{where,} \\ \bar{J}_{Col} = \epsilon \frac{\partial \bar{E}_{Col}}{\partial t} \end{cases} \quad (4)$$

- 3) The third one is the **Maxwell's vector potential**  $A_{Max}$ ;  $A_{Max}$  is induced by the variation of  $E_{Far}$  and  $E_{Max}$  as

$$\left. \begin{aligned} \nabla \times \vec{B}_{Max} &= \mu\epsilon \frac{\partial (\vec{E}_{Far} + \vec{E}_{Max})}{\partial t} \\ \vec{E}_{Far} &= -\frac{\partial \vec{A}_{Amp}}{\partial t} \\ \vec{E}_{Max} &= -\frac{\partial \vec{A}_{Max}}{\partial t} \end{aligned} \right\} \Rightarrow \nabla^2 \vec{A}_{Max} = -\mu\epsilon \frac{\partial^2 (\vec{A}_{Amp} + \vec{A}_{Max})}{\partial t^2} \quad (5)$$

Specified to the lumped-parameter electric circuits, three electric fields are generated by the charges passing through electric devices:

- 1) The Coulomb's fields are generated by the charges gathered at nodes. Those charges are pumped in and out by circuit devices.
- 2) The Faraday's fields are induced by the currents in wires. Those currents are regulated by circuit devices.
- 3) The Maxwell's fields are induced by the variation of all the electric fields. The variation of electric fields is modified by circuit devices.

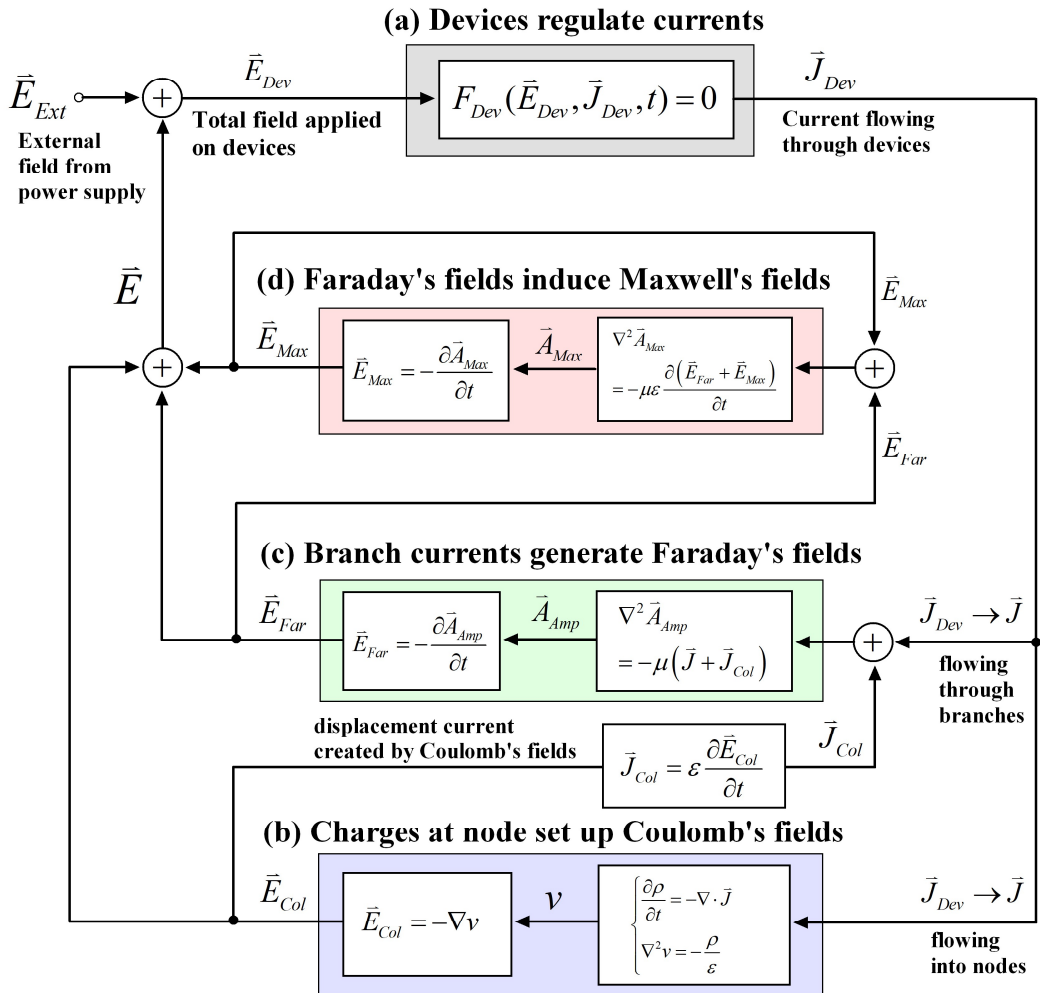


Fig. 3. Field components and their interactions with circuit devices in electric circuits.

The dynamics of charges in electric circuits are summarized in Fig. 3. The circuit

devices are elements, such as resistors, PN junctions, Josephson junctions, and Quantum-phase-slip (QPS) junctions, inside which, charges are driven by the electric field  $E_{Dev}$ , and passing through the device with a flow-rate  $J_{Dev}$ . The function of the electric device can be generally written as

$$F_{Dev}(E_{Dev}, J_{Dev}, t) = 0 \quad (6)$$

### B. Dynamics of circuit devices in lumped-parameter circuits

Lumped-parameter circuits assume that the circuit dimension is much smaller than the length of the electromagnetic waves, and the power of the electromagnetic radiation can be ignored, thus,  $A_{Max}$  in lumped-parameter circuits is neglected, namely

$$\vec{A}_{Max} \approx 0 \quad (7)$$

Accordingly, Fig. 3 is simplified as Fig. 4. In the model, electric devices are driven by  $E_{Dev}$  and pump charges with a flow-rate  $J_{Dev}$  to nodes. The  $E_{Dev}$  comes from the Coulomb's fields at nodes and the Faraday's fields in wires; the Coulomb's scalar potential at nodes and the vector potential  $A_{Amp}$  in wires are meanwhile set up by the charges passing through the devices.

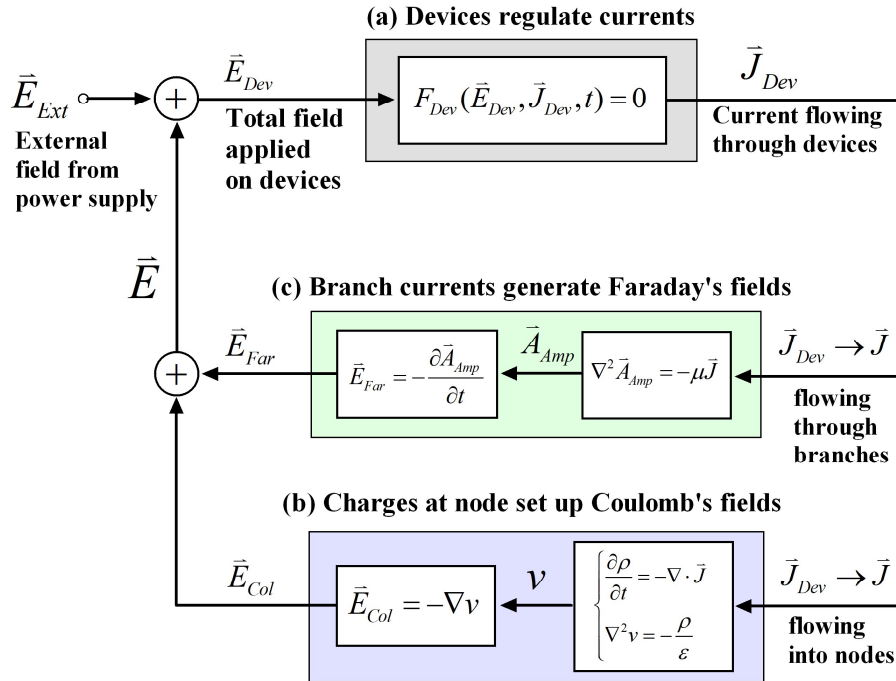


Fig. 4. System model of electric circuits, in which, circuit devices pump charges to nodes.

By reversing the signal directions, Fig. 4 can be also redrawn as Fig. 5. In this model, electric devices are driven by  $J_{Dev}$ , and generate the  $A_{Amp}$  in wires with a flow-rate  $E_{Dev}$ . The  $J_{Dev}$  is supplied by both the current that generates the  $A_{Amp}$  in wires, and the displacement current of the charges at nodes. The  $E_{Dev}$  of the device sets up the Faraday's fields in wires and the Coulomb's fields at nodes, like the counter-force.

Fig. 4 and 5 are the interaction models of electric devices with electromagnetic fields; they reveal that circuit devices work as either the electric-charge pumps (ECPs) [14] or

the magnetic-flux pumps (MFPs) [14] in electric circuits:

1) With  $E_{Dev}$  as input and  $J_{Dev}$  as output, the circuit device is a ECP that keep pumping charges from node to node with a flow-rate  $J_{Dev}$ . The input  $E_{Dev}$  is applied by the Coulomb's fields generated by the charges at nodes, and the Faraday's fields induced by the currents in wires.

2) With  $J_{Dev}$  as input and  $E_{Dev}$  as output, the circuit device is an MFP that keep charging fluxes into loops with a flow-rate  $E_{Dev}$ . The input  $J_{Dev}$  is supplied by the currents that preserve magnetic fields in wires, and the displacement currents induced by the Coulomb's fields at nodes.

Since electric devices have **two working modes**, one electric circuit will achieve **two dynamic models**, and two dynamic models exhibit the charge-flux duality of one electric circuit.

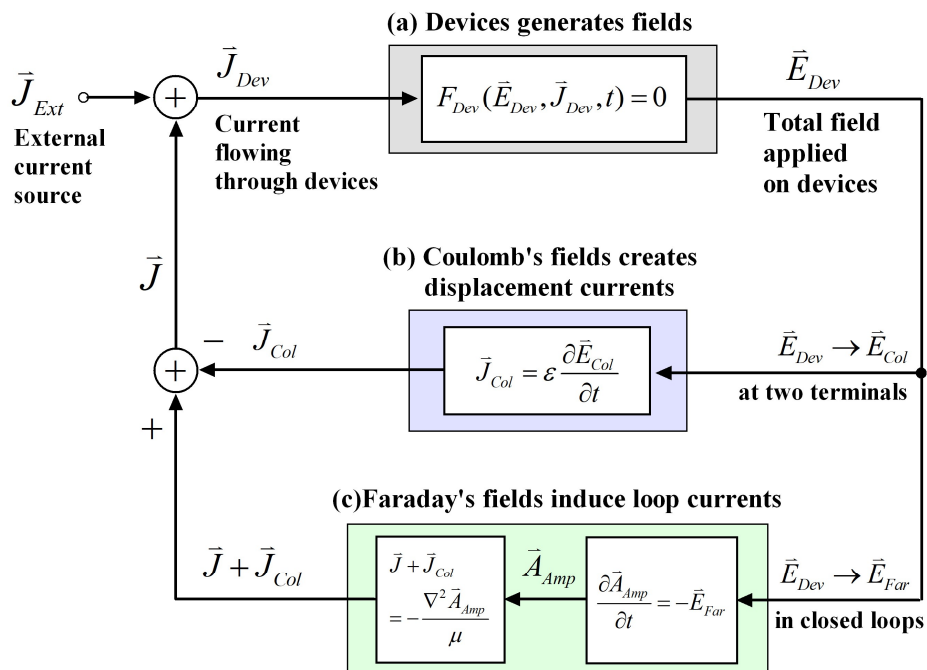


Fig. 5. System model of electric circuits, in which, circuit devices generate potentials to loops.

## 4. Electromagnetic-field-based circuit theory

### A. Charge-flux duality in one electric circuit

The charge-flux duality in one electric circuit is similar with the wave-particle duality of light, as illustrated in Fig. 6. From the view of electric field, a circuit is an **electric-charge distribution network**, where electric charges are flowing from node to node, and is also a **magnetic-flux distribution network**, where magnetic fluxes are transferred from loop to loop, from the view of magnetic field. Accordingly, a circuit is treated as an ECP network, if charges are the energy carriers, or an MFP network, if fluxes are the energy carriers.

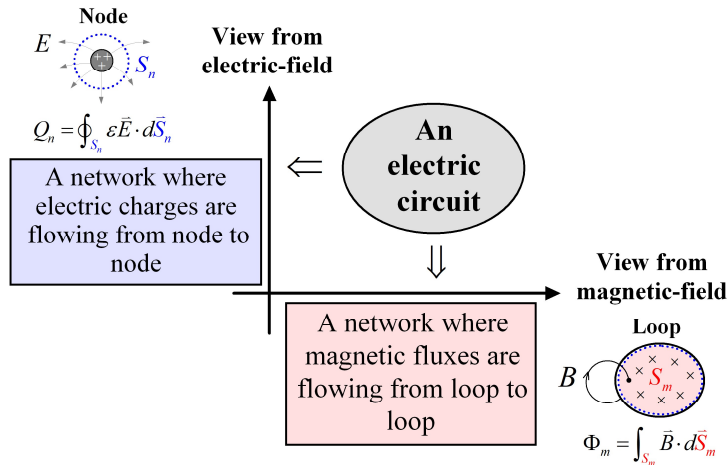


Fig. 6. Charge-flux duality in one electric circuit

For the lumped-parameter circuit analyses, the field components shown in Fig. 4 and 5 are implemented by four variables, as illustrated in Fig. 7.

1) **Charge ( $Q$ ) and voltage ( $v$ )** are the variables used in the **charge-based analysis** for ECP networks.

2) **Flux ( $\Phi$ ) and current ( $i$ )** are the variables used in the **flux-based analysis** for MFP networks.

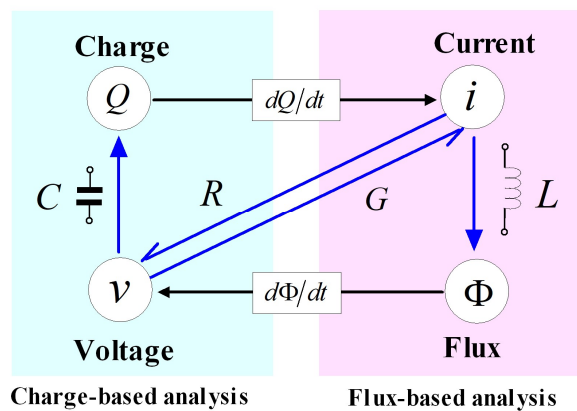


Fig. 7. Four variables used in circuit analyses.

## B. Charge-based circuit analysis

**If charges are the energy carriers, a circuit is modeled as the ECP network,** where the nodes that store charges with capacitances are the ECCs; the circuit devices that transfer charges to nodes are the ECPs.

The  $Q_n$  stored by an ECC is the flux of the electric fields thrusting through the surface of the node; it is defined by the integration of  $\rho$  as

$$Q_n = \oint_{S_n} \varepsilon \vec{E} \cdot d\vec{S}_n = \int_{V_n} \rho \cdot dV_n \quad (8)$$

The  $Q_n$  stored in the ECC creates a node voltage  $v_n$ ; the node voltages drive ECPs to pump charges in and out of nodes. The total charge passed through an ECP is recorded by  $Q_{cp}$ ; the **flow-rate** of  $Q_{cp}$  is accordingly the branch current  $i_{cp}$  of the ECP,

$$i_{cp} = \frac{dQ_{cp}}{dt} \quad (9)$$

With  $Q_{cp}$  as the output, the functions of both phase-independent and phase-dependent ECPs are defined with QVRs.

## C. Flux-based circuit analysis

**If fluxes are the energy carriers, a circuit is modeled as the MFP network,** where the loops that store fluxes with inductances are the MFCs; the circuit devices that generate fluxes in loops are the MFPs.

The  $\Phi_m$  coupled in an MFC is the flux of the magnetic fields thrusting through the surface of the loop; it is defined by the integration of  $A_{Amp}$  as

$$\Phi_m = \int_{S_m} \vec{B} \cdot d\vec{S}_m = \oint_{l_m} \vec{A}_{Amp} \cdot d\vec{l}_m \quad (10)$$

The  $\Phi_m$  stored in the MFC induces the loop current  $i_m$ ; the loop currents drive MFPs to generate positive or negative fluxes in loops. The total flux generated by an MFP is recorded by  $\Phi_{fp}$ ; the **flow-rate** of  $\Phi_{fp}$  is the two-terminal voltage  $v_{fp}$  of the MFP,

$$v_{fp} = \frac{d\Phi_{fp}}{dt} \quad (11)$$

With the  $\Phi_{fp}$  as the output, the functions of both phase-independent and phase-dependent MFPs are defined with FCRs.

## D. Example of ECP and MFP networks

The circuit example is shown in Fig. 8, where the wire has an inductance  $L_1$ ; the capacitance between two terminals is  $C_1$ ; the resistance of lamp is  $R_L$ . Fig. 8 is a schematic of the circuit, which has two equivalent circuits for circuit analysis.

The first equivalent circuit diagram is shown in Fig. 9(a), where the battery modeled with Thevenin's equivalent is a current source  $V_S$  in serial with a resistor  $R_S$ . The ECP network is shown in Fig. 9(b). The Thevenin's equivalent of the battery is defined as ECP-1, as shown in Fig. 9(c), and the resistor  $R_L$  is defined as ECP-2, as shown in Fig. 9(d). The Node-1 with the capacitor  $C_1$  is accordingly an ECC; the ECC stores the charges pumped in by ECP-1 and out by ECP-2.

The second equivalent circuit diagram is shown in Fig. 10(a), and the MFP network is shown in Fig. 10(b). The Norton's equivalent circuit of the battery is modeled as MFP-1, and the component of  $R_L$  and  $C_1$  in parallel is defined as MFP-2; the Loop-1

with inductance  $L_1$  is accordingly an MFC; the MFC preserves the magnetic-flux pumped in by MFP-1 and out by MFP-2.

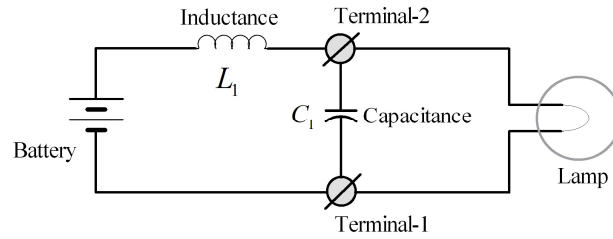


Fig. 8. An example circuit.

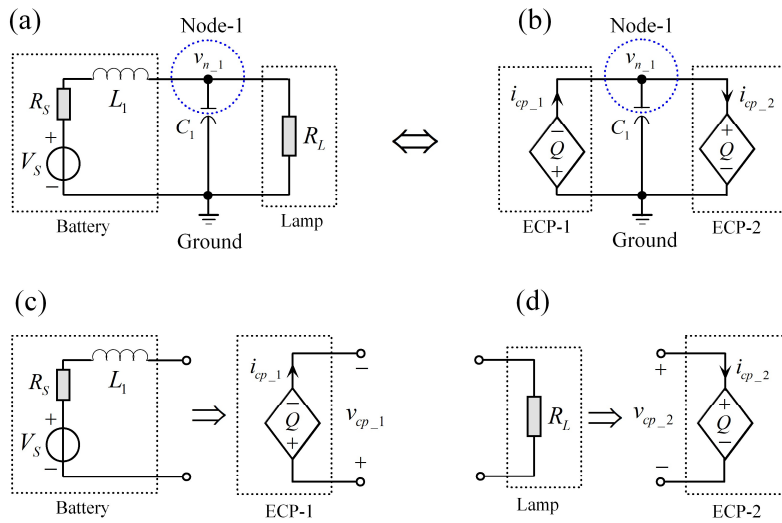


Fig. 9. Equivalent circuit of the example circuit: (a) circuit diagram with Thevenin's voltage model; (b) equivalent ECP network; (c) equivalent circuit of ECP-1; (d) equivalent circuit of ECP-2.

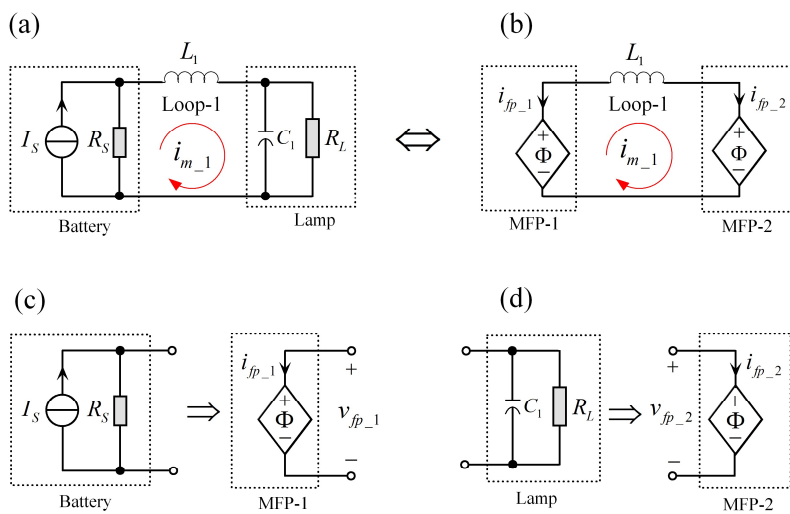


Fig. 10. Equivalent circuit of the example circuit: (a) circuit diagram with Norton's current model; (b) equivalent MFP network; (c) equivalent circuit of MFP-1; (d) equivalent circuit of MFP-2.



Therefore, an electric circuit can be modeled as an ECP network to implement a charge-based circuit analysis, or an MFP network to conduct a flux-based circuit analysis, depending on what kind of energy carrier (charge or flux) is used.

## 5. Charge-based circuit analysis

### A. Objects of ECP network

To conduct the **charge-based circuit analysis**, a given electric circuit is modeled as an ECP network, and is decomposed into a group of ECCs and ECPs, as shown in Fig. 11, where the number of ECCs is  $X$  and the number of ECPs is  $Y$ .

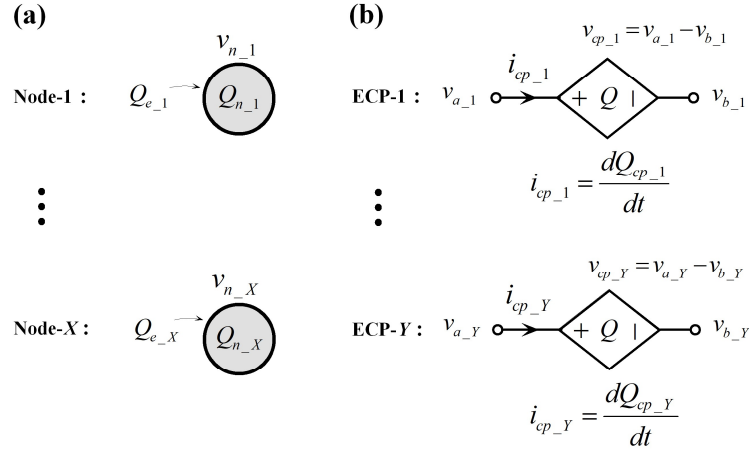


Fig. 11. Objects of ECP network: (a) Nodes also defined as ECCs; (b) ECPs.

(a)

$$\mathbf{C}_n = \begin{matrix} & \begin{matrix} \text{Node-1} & \cdots & \text{Node-X} \end{matrix} \\ \begin{matrix} \text{Node-1} \\ \vdots \\ \text{Node-X} \end{matrix} & \begin{bmatrix} c_{n_{11}} & \cdots & c_{n_{1X}} \\ \vdots & \cdots & \vdots \\ c_{n_{X1}} & \cdots & c_{n_{XX}} \end{bmatrix} \end{matrix} \quad c_{n_{ij}} = \begin{cases} C_{n_i}, & i = j : \text{total-capacitance of Node-}i \\ -C_{n_{ij}}, & i \neq j : \text{capacitance between Node-}i \text{ and Node-}j \end{cases}$$

(b)

$$\mathbf{L}_{cp} = \begin{matrix} & \begin{matrix} \text{ECP-1} & \cdots & \text{ECP-Y} \end{matrix} \\ \begin{matrix} \text{ECP-1} \\ \vdots \\ \text{ECP-Y} \end{matrix} & \begin{bmatrix} l_{cp_{11}} & \cdots & l_{cp_{1Y}} \\ \vdots & \cdots & \vdots \\ l_{cp_{Y1}} & \cdots & l_{cp_{YY}} \end{bmatrix} \end{matrix} \quad l_{cp_{ij}} = \begin{cases} L_{cp_i}, & i = j : \text{self-inductance of ECP-}i \\ -M_{cp_{ij}}, & i \neq j : \text{mutual-inductance between ECP-}i \text{ and ECP-}j \end{cases}$$

(c)

$$\boldsymbol{\sigma}_n = \begin{matrix} & \begin{matrix} \text{ECP-1} & \cdots & \text{ECP-Y} \end{matrix} \\ \begin{matrix} \text{Node-1} \\ \vdots \\ \text{Node-X} \end{matrix} & \begin{bmatrix} \sigma_{n_{11}} & \cdots & \sigma_{n_{1Y}} \\ \vdots & \cdots & \vdots \\ \sigma_{n_{X1}} & \cdots & \sigma_{n_{XY}} \end{bmatrix} \end{matrix} \quad \sigma_{n_{ij}} = \begin{cases} +1, & \text{if } v_{n_i} \text{ is imposed on the "+" terminal of ECP-}j \\ -1, & \text{if } v_{n_i} \text{ is imposed on the "-" terminal of ECP-}j \\ 0, & \text{otherwise} \end{cases}$$

Fig. 12. Circuit parameters of ECP network: (a) capacitance matrix of ECCs; (b) inductance matrix of ECPs; (d) incidence matrix of the connections between ECCs and ECPs.

1) For the Node- $i$  ( $i=1, \dots, X$ ) shown in Fig. 11(a),  $v_{n_i}$  is the node voltage, and  $Q_{n_i}$  is the charge contained in the ECC;  $Q_{e_i}$  is the charge induced to the node by external voltage sources.

2) For the ECP- $j$  ( $j=1, \dots, Y$ ) shown in Fig. 11(b),  $v_{cp\_j}$  is the two-terminal voltage;  $Q_{cp\_j}$  records the charges flowing through the ECP,  $i_{cp\_j}$  is accordingly the flow-rate of charges passed through ECP- $j$ .

### B. Electric-charge containers

**The ECCs are the nodes coupled through mutual capacitances.** The self and mutual capacitances of ECCs are defined in the capacitance matrix  $C_n$ , as shown in Fig. 12(a). The charges stored in ECCs are preserved by the nodal voltages as

$$\mathbf{Q}_n = \mathbf{C}_n \cdot \mathbf{v}_n - \mathbf{Q}_e \quad (12)$$

where the state vectors of ECCs are defined as

$$\begin{cases} \mathbf{v}_n = [v_{n\_1} \ \dots \ v_{n\_X}]^T \\ \mathbf{Q}_n = [Q_{n\_1} \ \dots \ Q_{n\_X}]^T \\ \mathbf{Q}_e = [Q_{e\_1} \ \dots \ Q_{e\_X}]^T \end{cases} \quad (13)$$

### C. Electric-charge pumps

**The nodal voltages of ECCs are applied to the terminals of ECPs, and ECPs pump charges in and out of the ECCs.** For ECP- $k$  shown in Fig. 13(a), its internal structure is illustrated in Fig. 13(b), where charge-pump elements (CPEs) are connected in serials (the number of CPEs is  $Z_k$ ) to transfer the same number of charges  $Q_{cp\_k}$ . CPEs are basic elements, such as resistors, PN junctions, QPS voltages; each of them is defined with a QVR, as illustrated in Fig. 14.

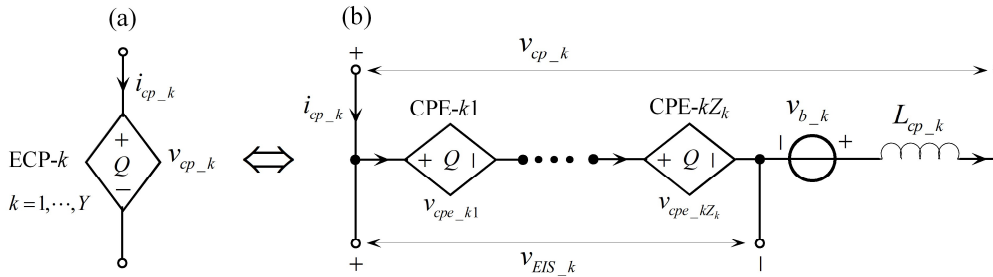


Fig. 13. Structure of ECP: (a) symbol of ECP (b) components inside ECP.

In the ECP- $k$ , CPEs bear an elements-in-serial (EIS) voltage  $v_{EIS\_k}$  to transfer the same  $Q_{cp\_k}$ , and  $v_{EIS\_k}$  is sum of the two-terminal voltages of CPEs. Accordingly, the QVR of the CPEs in serial is

$$\begin{cases} Q_{cp\_k} = Q_{cpe\_1} \ \dots \ = Q_{cpe\_Z_k} \\ v_{EIS\_k} = \sum_{j=1}^{Z_k} v_{cpe\_j} \end{cases} \quad (14)$$

This  $v_{EIS\_k}$  is supplied by three potentials:

- 1) The first one is  $v_{cp}$ ; it is the potential applied by the nodal voltages;
- 2) The second one is  $v_{b\_k}$ ; it is the external voltage source;
- 3) The third one is the electromagnetic forces induced by the magnetic fields inside

and between ECPs.

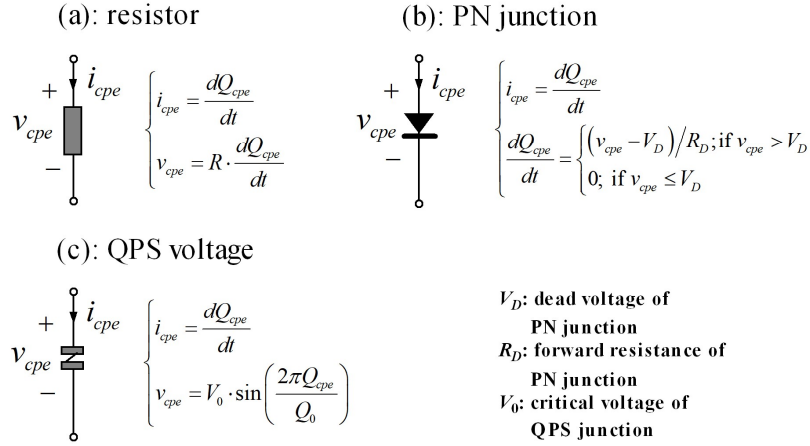


Fig. 14. Typical charge-pump elements: (a) resistor; (b) PN junction; (c) QPS junction.

**ECPs are coupled through mutual inductances.** The self and mutual inductances of ECPs are described by the inductance matrix  $\mathbf{L}_{cp}$ , as shown in Fig. 12(b). The  $L_{cp\_k}$  is the self-inductance of ECP- $k$ ; the  $M_{cp\_jk}$  is the mutual-inductance between ECP- $j$  and ECP- $k$ , as illustrated in Fig. 15.

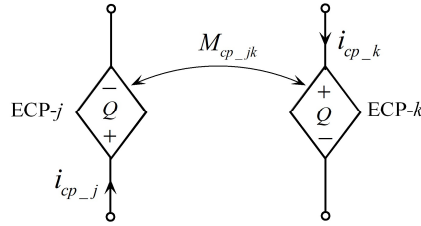


Fig. 15. Mutual-inductance between two ECPs.

Four state vectors for ECPs are defined as

$$\begin{cases} \mathbf{v}_{cp} = [v_{cp\_1} \ \cdots \ v_{cp\_Y}]^T \\ \mathbf{Q}_{cp} = [Q_{cp\_1} \ \cdots \ Q_{cp\_Y}]^T \\ \mathbf{v}_{EIS} = [v_{EIS\_1} \ \cdots \ v_{EIS\_Y}]^T \\ \mathbf{v}_b = [v_{b\_1} \ \cdots \ v_{b\_Y}]^T \end{cases} \quad (16)$$

Accordingly, the function of ECPs in matrix is written as

$$\mathbf{v}_{EIS} = \mathbf{v}_b + \mathbf{v}_{cp} - \mathbf{L}_{cp} \cdot \frac{d^2 \mathbf{Q}_{cp}}{dt^2} \quad (15)$$

Since each CPE shown in Fig. 14 has a specific QVR, we can always have the QVR of CPEs in (14) written in matrix as

$$F_{EIS}(\mathbf{v}_{EIS}, \mathbf{Q}_{cp}, t) = 0 \quad (17)$$

The QVR for specific CPE is illustrated in Fig. 14.

#### D. Interactions between ECCs and ECPs

**The connections between ECCs and ECPs** are described by  $\sigma_n$  defined in Fig. 12(c). The positive terminal of ECP- $k$  is connected at Node- $x$  for  $\sigma_{n_{xk}} = 1$ , and the negative terminal is connected at Node- $y$  for  $\sigma_{n_{yk}} = -1$ , as illustrated in Fig. 16. For the ECPs that have only one terminal connected to Node- $i$  ( $i = 1, \dots, X$ ), their second terminals are assumed to be connected to the ground.

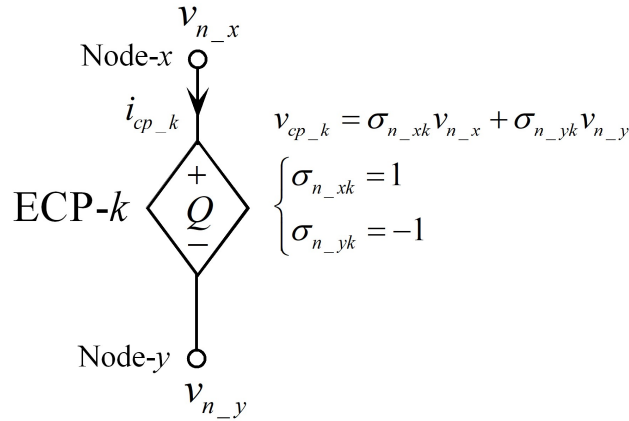


Fig. 16. Connections of an ECP at nodes

**The interactions between ECPs and ECCs** are described by two equations:

First, the ECPs are driven by the nodal voltages, then the voltages at two terminals of ECPs are expressed by nodal voltages as

$$\mathbf{v}_{cp} = \boldsymbol{\sigma}_n^T \cdot \mathbf{v}_n \quad (18)$$

Second, ECPs pump charges in and out of ECCs, and the charges contained in nodes comply with the charge-conservation law (CCL) as

$$\mathbf{Q}_n + \boldsymbol{\sigma}_n \cdot \mathbf{Q}_{cp} = \mathbf{Q}_{const} \quad (19)$$

where  $\mathbf{Q}_{const} = [Q_{const_1} \dots Q_{const_X}]^T$  is the constant vector of ECCs.

#### E. General system model of ECP networks

**An interaction system model of ECPs and ECCs** is drawn by synthesizing all the circuit equations of ECP network, as shown in Fig. 17. In this model:

- 1) The ECPs are driven by nodal voltages and external voltage sources, and pump charges to ECCs.
- 2) The ECCs store charges with capacitances, and turn the charges linearly into nodal voltages, like charge-voltage convertors.
- 3) The charge and energy exchanges between ECPs and ECCs comply with the CCL and the energy-conservation law; the CCL is a kind of mass conservation law.

Therefore, the flux-based analysis will model any given circuit as an ECP network, and the ECP network will finally be described by the system model shown in Fig. 17 and the parameters summarized in Table 3.

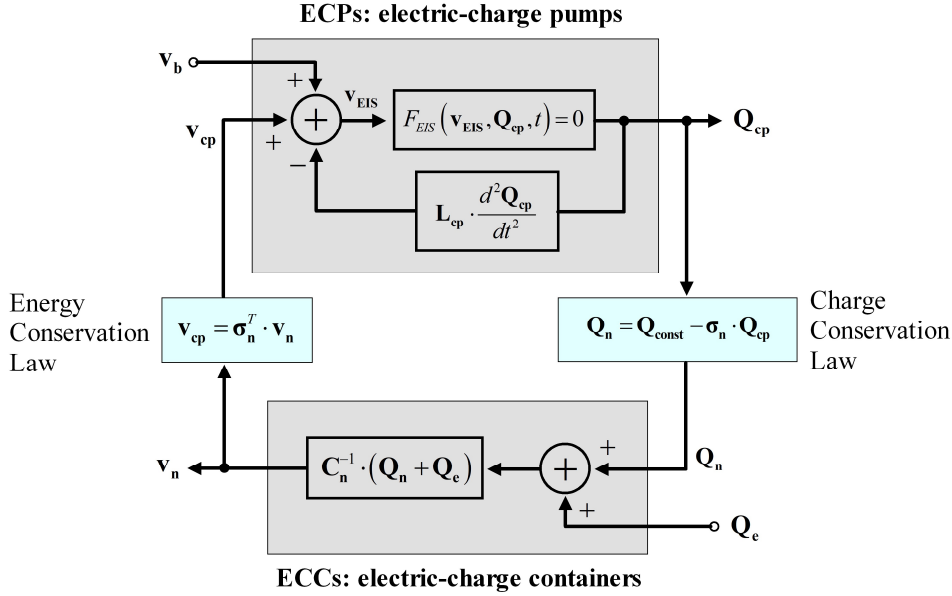


Fig. 17. General system model of ECP networks.

Table 3. Circuit descriptions of ECP network

	Variables
<b>Inputs</b>	$v_b$ : external voltage sources applied to ECPs $Q_e$ : external charges applied to ECCs
<b>Outputs</b>	$v_n$ : nodal voltages at ECCs $Q_{cp}$ : charges flowing through ECPs
<b>Interactions</b>	$\sigma_n$ : incidence matrix between ECPs and ECCs $C_n$ : self and mutual capacitances of ECCs $L_{cp}$ : self- and mutual inductances of ECPs
<b>Devices</b>	$F_{EIS}(v_{EIS}, Q_{cp}, t) = 0$ : QVR of CPEs in searl inside ECPs

#### F. Electric-charge-flow diagram

**Electric-charge flow (ECF) diagram is the interaction diagram for ECP networks.** It is the graphical expression of the system model in Fig. 17. The symbols of objects and their connections are exhibited in Fig. 18:

1) A node (ECC) is symbolized with a circle shown in Fig. 18(a); the ground, which is the datum node, is represented with the symbol shown in Fig. 18(b).

2) An ECP is implemented with a brick-shape block shown in Fig. 18(c).

The non-zero elements of  $\sigma_n$ ,  $C_n$ ,  $L_{cp}$  are transformed into the directed lines connected between ECPs and ECCs, as illustrated Fig. 18(d).

1) The non-zero elements of  $\sigma_n$  are turned into the directed lines connected between ECPs and nodes. The arrow indicates the direction of flows in ECPs.

2) The non-zero elements of  $C_n$  are expressed by the double-arrow lines connected between two nodes; the two arrows are pointing to the nodes.

3) The non-zero elements in  $L_{cp}$  are implemented by the double-arrow lines connected between two ECPs; the two arrows are pointing to the ECPs.

Furthermore, the non-zero elements in  $\mathbf{v}_b$  are implemented by the input arrows pointing to ECPs, while the non-zero elements in  $(\mathbf{Q}_e + \mathbf{Q}_{const})$  are represented with the input arrows pointing to nodes. The connections of objects in ECF diagrams are summarized in Table 4.

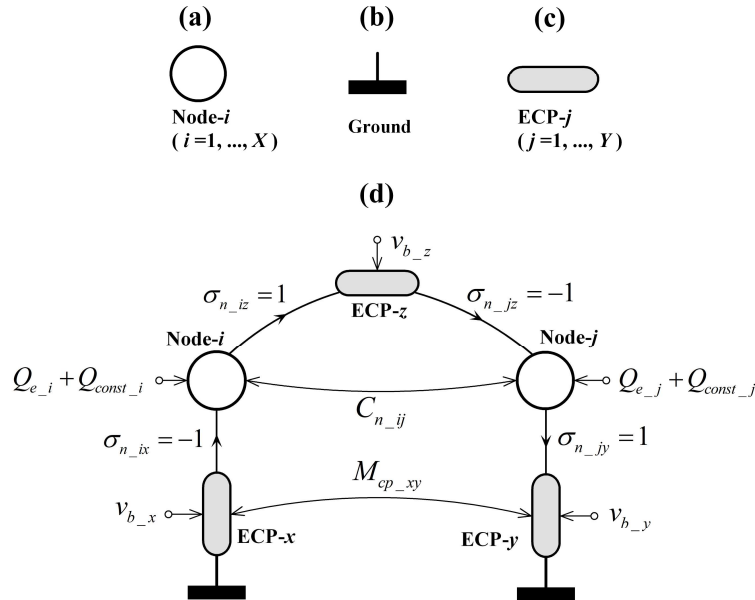


Fig. 18. ECF diagram: (a) symbol of nodes; (b) symbol for the datum node; (c) symbol of ECPs; (d) an example ECF diagram.

Table 4. Elements in matrices and their entities in ECF diagrams

Matrix	Element	Entity in MFF diagram
$\sigma_n$	$\sigma_{n_xk} = 1$	A directed line connected between Node- $x$ and ECP- $k$ , with the arrow leaving Node- $x$ .
	$\sigma_{n_yk} = -1$	A directed line connected between Node- $y$ and ECP- $k$ , with the arrow entering Node- $y$ .
$C_n$	$C_{n_i} = 1$	The self-capacitance of Node- $i$ .
	$C_{n_{ij}} = -1$	A double arrow line with a weight of $C_{n_{ij}}$ ; it is connected between Node- $i$ and Node- $j$ ; its two arrows are pointing to Node- $i$ and Node- $j$ .
$L_{cp}$	$L_{cp_k}$	The self-inductance of ECP- $k$ .
	$M_{cp_{jk}}$	A double arrow line with a weight of $M_{cp_{jk}}$ ; it is connected between ECP- $j$ and ECP- $k$ ; its two arrows are pointing to ECP- $i$ and ECP- $j$ .
$\mathbf{v}_b$	$v_{b_k}$	A input for ECP- $k$ , with a value of $v_{b_k}$ .
$\mathbf{Q}_e + \mathbf{Q}_{const}$	$Q_{e_i} + Q_{const_i}$	A input for Node- $i$ , with a value of $Q_{e_i} + Q_{const_i}$ .

The application of ECF diagram is demonstrated in the following analyses of PN-junction circuits. By tracing the charges stored in nodes, an ECF diagram can vividly depicts how ECPs transfer charges from node to node, how two ECPs are interacting

through mutual inductance, and how two ECCs are interacting through mutual capacitances.

*G. ECF diagram of PN-junction circuits*

A voltage-biased PN junction shown in Fig. 19(a) is as an ECP, which is a diode in transferring electric charges. It keeps pumping electric charges when the two-terminal voltage exceeds the threshold voltage  $V_{TH}$ , as shown in Fig. 19(b), where the threshold voltage  $V_{TH}$  is adjusted by the bias voltage, namely,  $V_{TH} = V_D - v_b$ . In the following circuit analyses, the voltage-biased PN junctions is symbolized as shown in Fig. 19(c), for simplicity.

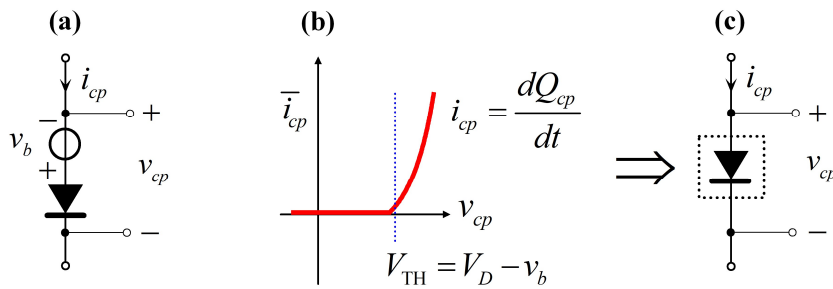


Fig. 19. PN junctions working as ECP: (a) a voltage-biased PN junction; (b) the current-voltage characteristic; (c) a symbol for voltage-biased PN junctions.

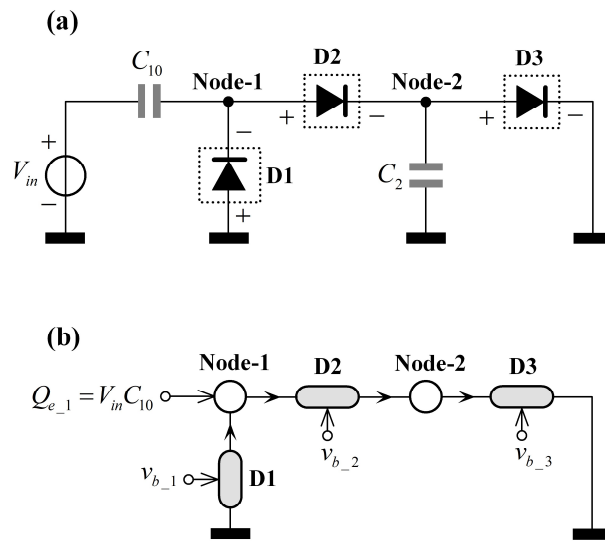


Fig. 20. (a) A PN-junction circuit and its (b) ECF diagram.

Fig. 20(a) shows a charge-pump circuit implemented with the voltage-biased PN junctions; this PN junction circuit will pump charges from Node-1 to Node-2, under the driving of the clock signal  $V_{in}$ .

The ECF diagram of the PN-junction circuit is shown in Fig. 20(b). It vividly depicts the charge-pumping principles, as illustrated in Fig. 21.

1) A negative  $V_{in}$  induces an external charge  $Q_{e-1}$  to Node-1, and lowers the nodal voltage at Node-1, as shown in Fig. 21(a); the low voltage will turn on the junction D1 to pump charges to Node-1.



2) With charges filling in Node-1, the voltage at Node-1 will increase to turn off the diode D1, as exhibited in Fig. 21(b).

3) When the voltage  $V_{in}$  returns to zero, the voltage at Node-1 will turn on the junction D2 to pipe the charges from Node-1 to Node-2, as depicted in Fig. 21(c).

4) Charges filling in Node-2 will further turn on the junction D3 to pipe the charges from Node-2 to the ground, as illustrated in Fig. 21(d).

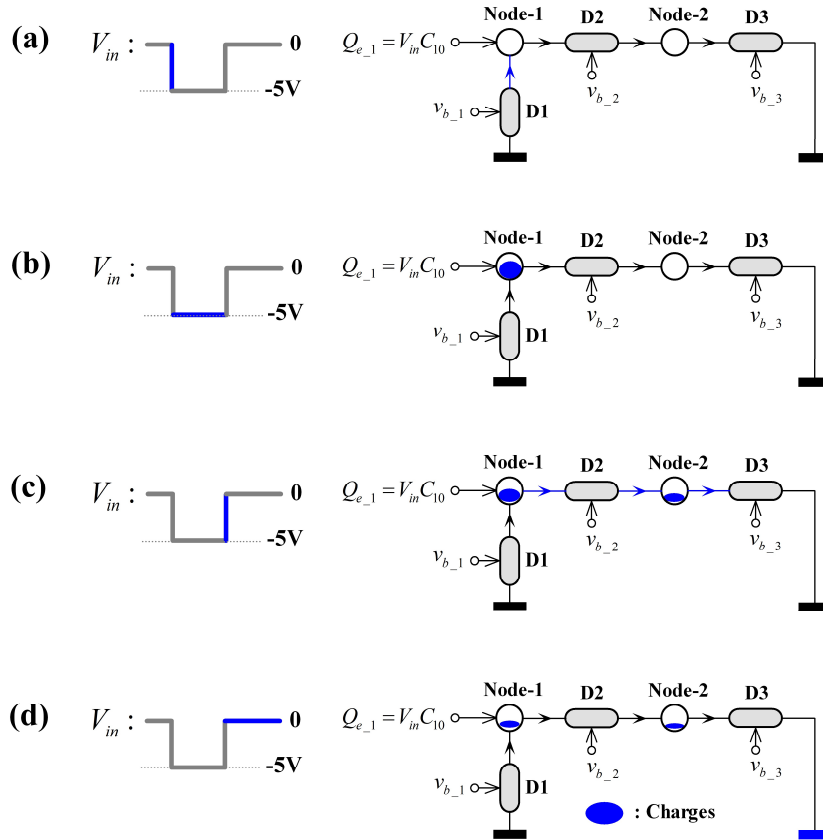


Fig. 21. Working principle of a PN-junction circuit depicted by ECP diagram. (a) voltage of Node-1 is lowered to turn on D1, when  $V_{in}$  is pulled from 0V to -5V; (b) D1 pumps charges into Node-1, until it is turned off by the increasing voltage of Node-1; (c) D2 is turned on to pipe the charges to Node-2, when  $V_{in}$  is returned to 0V; (d) D3 is turned on to pipe charges in Node-2 to ground, until node voltages turn the diodes off.

## 6. Flux-based circuit analysis

### A. Objects of MFP network

To conduct the **flux-based circuit analysis**, we can redraw the given electric circuit as an MFP network, and extract all the MFCs and MFPs, as shown in Fig. 22, where  $X$  is the number of loops and  $Y$  is the number of MFPs.

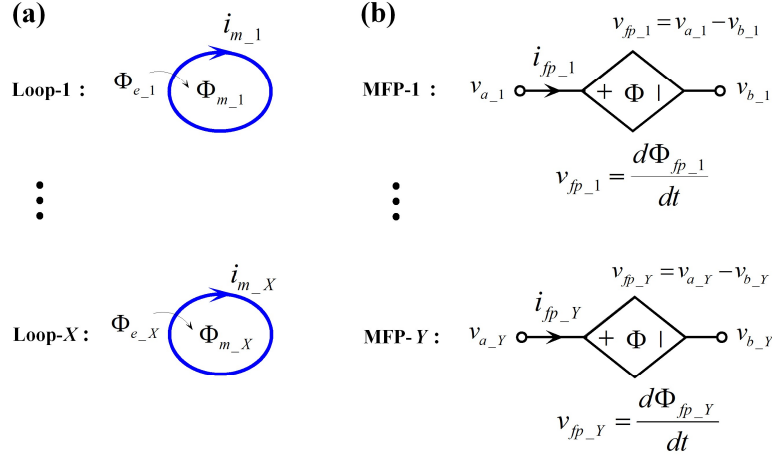


Fig. 22. Objects of ECP network: (a) Loops also known as MFCs; (b) MFPs.

(a)

$$\mathbf{L}_m = \begin{matrix} & \begin{matrix} \text{Loop-1} & \cdots & \text{Loop-X} \end{matrix} \\ \begin{matrix} \text{Loop-1} \\ \vdots \\ \text{Loop-X} \end{matrix} & \begin{bmatrix} l_{m_11} & \cdots & l_{m_1X} \\ \vdots & \cdots & \vdots \\ l_{m_X1} & \cdots & l_{m_{XX}} \end{bmatrix} \end{matrix} \quad l_{m_{ij}} = \begin{cases} L_{m_i}, & i = j : \text{self-inductance of Loop-}i \\ -M_{m_{ij}}, & i \neq j : \text{mutual-inductance between Loop-}i \text{ and Loop-}j \end{cases}$$

(b)

$$\mathbf{C}_{fp} = \begin{matrix} & \begin{matrix} \text{MFP-1} & \cdots & \text{MFP-Y} \end{matrix} \\ \begin{matrix} \text{MFP-1} \\ \vdots \\ \text{MFP-Y} \end{matrix} & \begin{bmatrix} c_{fp_11} & \cdots & c_{fp_1Y} \\ \vdots & \cdots & \vdots \\ c_{fp_Y1} & \cdots & c_{fp_{YY}} \end{bmatrix} \end{matrix} \quad c_{fp_{ij}} = \begin{cases} C_{fp_i}, & i = j : \text{inner-capacitance of MFP-}i \\ -C_{fp_{ij}}, & i \neq j : \text{capacitance between MFP-}i \text{ and MFP-}j \end{cases}$$

(c)

$$\boldsymbol{\sigma}_m = \begin{matrix} & \begin{matrix} \text{MFP-1} & \cdots & \text{MFP-Y} \end{matrix} \\ \begin{matrix} \text{Loop-1} \\ \vdots \\ \text{Loop-X} \end{matrix} & \begin{bmatrix} \sigma_{m_11} & \cdots & \sigma_{m_1Y} \\ \vdots & \cdots & \vdots \\ \sigma_{m_X1} & \cdots & \sigma_{m_{XY}} \end{bmatrix} \end{matrix} \quad \sigma_{m_{ij}} = \begin{cases} +1, & \text{if } i_{m_i} \text{ enters the "+" terminal of MFP-}j \\ -1, & \text{if } i_{m_i} \text{ enters the "-" terminal of MFP-}j \\ 0, & \text{otherwise} \end{cases}$$

Fig. 23. Circuit parameters of MFP network: (a) inductance matrix of MFCs; (b) capacitance matrix of MFPs; (c) incidence matrix of the connections of between MFCs and MFPs.

1) For the Loop- $i$  ( $i=1, \dots, X$ ) shown in Fig. 22(a),  $i_{m_i}$  is the mesh current;  $\Phi_{m_i}$  is the flux coupled by the MFC;  $\Phi_{e_i}$  is the external flux applied by external current sources or the magnetic dipoles coupled with the loop.

2) For the MFP- $j$  ( $j=1, \dots, Y$ ) shown in Fig. 22(b),  $i_{fp\_j}$  is the branch-current;  $\Phi_{fp\_j}$  records the magnetic-flux contributed by MFP- $j$  in loops;  $v_{fp\_j}$  is accordingly the flow-rate of fluxes generated by MFP- $j$ .

### B. Magnetic-flux containers

**MFCs are the loops coupled through mutual inductances.** The inductances of MFCs are defined by the inductance matrix  $\mathbf{L}_m$ , as shown in Fig. 23(a). The fluxes stored in MFCs are preserved by the loop currents as

$$\Phi_m = \mathbf{L}_m \cdot \mathbf{i}_m - \Phi_e \quad (20)$$

where the state vectors of MFCs are defined as

$$\begin{cases} \mathbf{i}_m = [i_{m\_1} \ \dots \ i_{m\_X}]^T \\ \Phi_m = [\Phi_{m\_1} \ \dots \ \Phi_{m\_X}]^T \\ \Phi_e = [\Phi_{e\_1} \ \dots \ \Phi_{e\_X}]^T \end{cases} \quad (21)$$

### C. Magnetic-flux pumps

**Loops currents of MFCs are applied to MFPs, and MFPs generate positive or negative fluxes in MFCs.** For the MFP- $k$  shown in Fig. 24(a), its general structure is exhibited in Fig. 24(b), where flux-pump elements (FPEs) are connected in parallel (the number of FPEs is  $Z_k$ ) to generate the same number of  $\Phi_{fp\_k}$ . The FPEs are basic elements, such as resistors, PN junctions, Josephson currents. Typical FPEs and their FCRs are seen in Fig. 25.

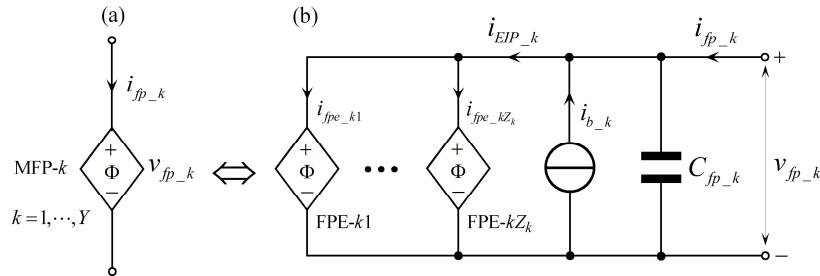


Fig. 24. Structure of MFP: (a) a symbol of MFP (b) components inside MFP.

In MFP- $k$ , FPEs generate the same output  $\Phi_{fp\_k}$  by absorbing the elements-in-parallel (EIP) current  $i_{EIP\_k}$ ; the  $i_{EIP\_k}$  is total currents shunted by FPEs. Accordingly, the FCR of the FPEs in parallel is expressed as

$$\begin{cases} \Phi_{fp\_k} = \Phi_{fpe\_k1} \ \dots = \Phi_{fpe\_kZ_k} \\ i_{EIP\_k} = \sum_{j=1}^{Z_k} i_{fpe\_j} \end{cases} \quad (22)$$

This  $i_{EIP\_k}$  is supplied by three kinds of currents:

- 1) The first one is  $i_{fp}$ ; it is the branch current supplied by loop currents;
- 2) The second one is  $i_{b\_k}$ , it is the externally applied current source;
- 3) The third one is the displacement current induced by the electric fields inside and

between MFPs.

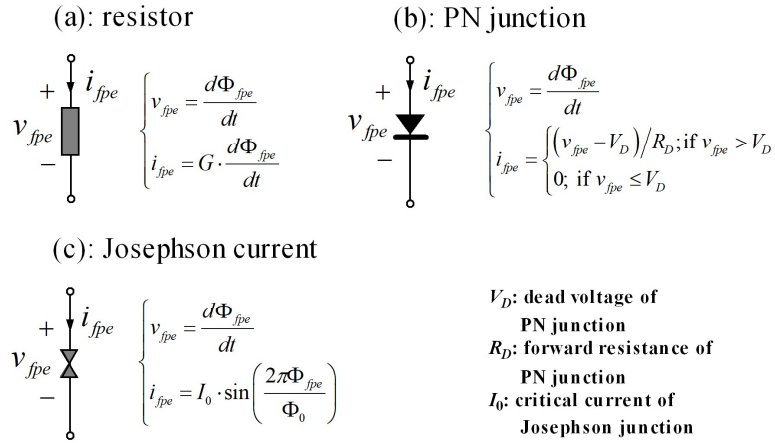


Fig. 25. Typical flux-pump elements: (a) resistor; (b) PN junction; (c) Josephson junction.

**MFPs are coupled through mutual capacitances.** The capacitances of MFPs are defined by the capacitance matrix  $\mathbf{C}_{fp}$  shown in Fig. 23(b). The  $C_{fp\_k}$  is the self-capacitance inside MFP- $k$ ; the  $C_{fp\_jk}$  is the mutual-capacitance between MFP- $j$  and MFP- $k$ , as illustrated in Fig. 26.

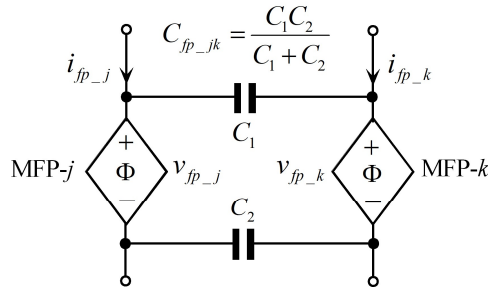


Fig. 26. Mutual-capacitance between two MFPs.

Four state vectors of MFPs are defined as

$$\begin{cases} \mathbf{i}_{fp} = [i_{fp\_1} \ \cdots \ i_{fp\_Y}]^T \\ \Phi_{fp} = [\Phi_{fp\_1} \ \cdots \ \Phi_{fp\_Y}]^T \\ \mathbf{i}_{EIP} = [i_{EIP\_1} \ \cdots \ i_{EIP\_Y}]^T \\ \mathbf{i}_b = [i_{b\_1} \ \cdots \ i_{b\_Y}]^T \end{cases} \quad (23)$$

The function in matrix for all the MFPs is written as

$$\mathbf{i}_{EIP} = \mathbf{i}_b + \mathbf{i}_{fp} - \mathbf{C}_{fp} \cdot \frac{d^2 \Phi_{fp}}{dt^2} \quad (24)$$

Since each FPE shown in Fig. 25 has a specific FCR, the FCR of FPEs in (22) can be generally written in matrix as

$$F_{EIP}(\mathbf{i}_{EIP}, \Phi_{fp}, t) = 0 \quad (25)$$

#### D. Interactions between MFCs and MFPs

The connections between MFCs and MFPs are described by  $\sigma_m$  in Fig. 23(c). As illustrated in Fig. 27, loop currents  $i_{m\_x}$  and  $i_{m\_y}$  flow in the positive terminal of MFP- $k$ , due to  $\sigma_{m\_xk} = 1$  and  $\sigma_{m\_yk} = 1$ , while the  $i_{m\_z}$  flows from in the negative terminal of MFP- $k$ , for  $\sigma_{m\_zk} = -1$ . The MFPs that are inserted in only one MFCs, are also assumed to be inserted in the outer-loop.

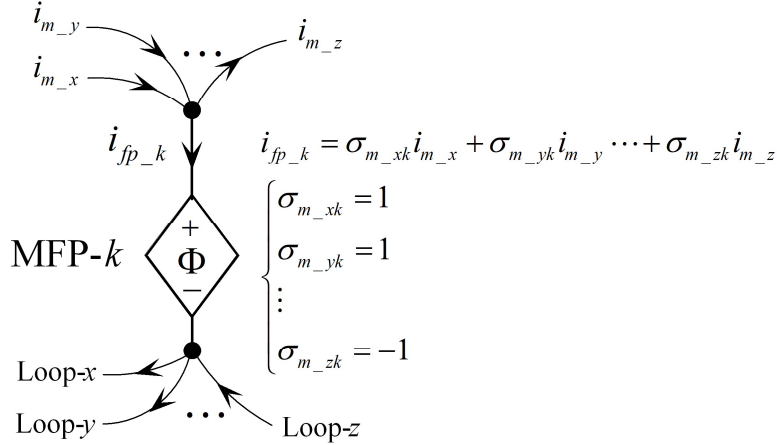


Fig. 27. Connections of an MFP in loops.

The interactions between MFPs and MFCs are described by two equations:

First, the MFPs are supplied by the loop currents, then the branch currents of MFPs are expressed with loop currents as

$$\mathbf{i}_{fp} = \boldsymbol{\sigma}_m^T \cdot \mathbf{i}_m \quad (26)$$

Second, MFPs pump fluxes in and out of MFCs, and the fluxes contained in loops must comply with the flux-conservation law (FCL) as

$$\boldsymbol{\Phi}_m + \boldsymbol{\sigma}_m \cdot \boldsymbol{\Phi}_{fp} = \boldsymbol{\Phi}_{const} \quad (27)$$

where  $\boldsymbol{\Phi}_{const} = [\Phi_{const\_1} \dots \Phi_{const\_X}]^T$  is the constant vector of MFCs.

#### E. General system model of MFP networks

An interaction system model of MFPs and MFCs is drawn by combining the circuit equations of MFP networks, as shown in Fig. 28.

1) The MFPs are driven by the loop currents and the external current sources, and pump magnetic fluxes to MFCs.

2) The MFCs preserve the fluxes with inductances, and turn the fluxes linearly into loop currents, like flux-current convertors.

3) MFPs and MFCs exchange magnetic fluxes and energies based on the FCL and the energy-conservation law; the FCL is a kind of mass conservation law.

In the flux-based circuit analysis, a given circuit is modeled as an MFP network, is completely described by the system model shown in Fig. 28 and the parameters summarized in Table 5.

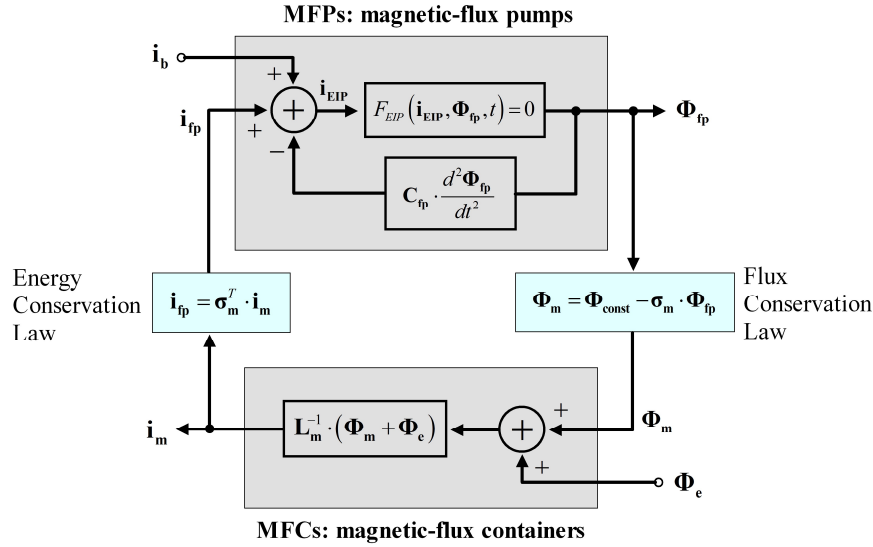


Fig. 28. General system diagram of MFP networks.

Table 5. Circuit descriptions of MFP network

	Variables
<b>Inputs</b>	$i_b$ : external current sources applied to MFPs $\Phi_e$ : external flux applied to MFCs
<b>Outputs</b>	$i_m$ : mesh currents inside MFCs $\Phi_{fp}$ : fluxes generated by MFPs
<b>Interactions</b>	$\sigma_m$ : incidence matrix between MFPs and MFCs $L_m$ : self and mutual inductances of MFCs $C_{fp}$ : self- and mutual capacitances of MFPs
<b>Devices</b>	$F_{EIP}(i_{EIP}, \Phi_{fp}, t) = 0$ : FCR of devices inside MFPs

### F. Magnetic-flux-flow diagram

**Magnetic-flux flow (MFF) diagram is the interaction diagram of MFP networks.** It is the graphical expression of the system model in Fig. 28. The objects and their connections for MFF diagrams are described in Fig. 29:

- 1) An MFC is symbolized with a circle shown in Fig. 29(a);
- 2) The outer-loop with its loop-current fixed as zero, is represented with the symbol shown in Fig. 29(b).

3) An MFP is implemented with a brick-shape block shown in Fig. 29(c).

The non-zero elements in  $\sigma_m$ ,  $L_m$ ,  $C_{fp}$  are turned into the connections between MFPs and MFCs, as illustrated in Fig. 29(d).

1) The non-zero elements of  $\sigma_m$  are turned into the directed lines connected between MFPs and MFCs. The arrow indicates the MFF direction of MFCs

2) The non-zero elements of  $L_m$  are expressed by the double-arrow lines connected between two MFCs; the two arrows are pointing to MFCs.

3) The non-zero elements in  $C_{fp}$  are implemented by the double-arrow lines connected between two MFPs; the two arrows are pointing to the MFPs.

Moreover, the non-zero elements in  $\mathbf{i}_b$  are implemented by the input arrows pointing to MFPs, while the non-zero elements in  $(\Phi_e + \Phi_{\text{const}})$  are represented with the input arrows pointing to MFCs. Details of those connections are seen in Table 6.

In MFF diagrams, the MFPs that have only one terminal connected to Loop- $i$  ( $i=1, \dots, X$ ), will have their second terminals connected to the outer-loop.

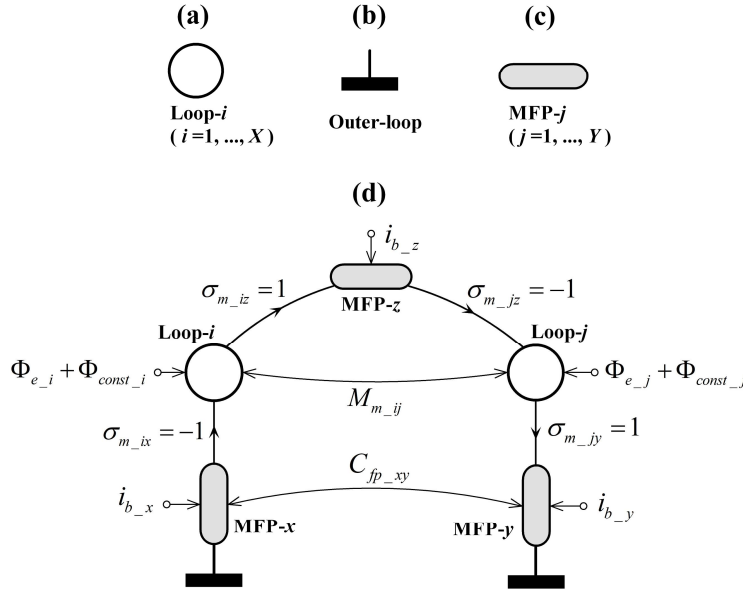


Fig. 29. MFF diagram: (a) symbol of MFCs; (b) symbol for the outer-loop; (c) symbol of MFPs; (d) an example MFF diagram.

Table 6. Elements in matrices and their entities in ECF diagrams

Matrix	Element	Entity in MFF diagram
$\sigma_m$	$\sigma_{m_xk} = 1$	A directed line connected between Loop- $x$ and MFP- $k$ , with the arrow leaving Loop- $x$ .
	$\sigma_{m_yk} = -1$	A directed line connected between Loop- $y$ and MFP- $k$ , with the arrow entering Loop- $y$ .
$L_m$	$L_{m_i} = 1$	The self-inductance of Loop- $i$ .
	$M_{m_{ij}} = -1$	A double arrow line with a weight of $M_{m_{ij}}$ ; it is connected between Loop- $i$ and Loop- $j$ , with its two arrows pointing to Loop- $i$ and Loop- $j$ .
$C_{fp}$	$C_{fp_k}$	The self-capacitance inside MFP- $k$ .
	$C_{fp_{jk}}$	A double arrow line with a weight of $C_{fp_{jk}}$ ; it is connected between MFP- $j$ and MFP- $k$ , with its two arrows pointing to MFP- $i$ and MFP- $j$ .
$\mathbf{i}_b$	$i_{b_k}$	A input to MFP- $k$ , with a value of $i_{b_k}$ .
$\Phi_e + \Phi_{\text{const}}$	$\Phi_{e_i} + \Phi_{\text{const}_i}$	A input to Loop- $i$ , with a value of $\Phi_{e_i} + \Phi_{\text{const}_i}$ .

The application of MFF diagram is demonstrated in the following analyses of Josephson junction circuits. By tracing the fluxes coupled in loops, we can vividly see from the MFF diagram how MFPs transfer fluxes from loop to loop, how two MFPs

are interacting through mutual capacitances, and how two ECCs are interacting through mutual inductances.

### G. MFF diagram of Josephson junction circuits

Dual to the voltage-biased PN junction, a current-biased Josephson junction shown in Fig. 30(a) is an MFP that works as a diode in transferring magnetic fluxes. It keeps pumping magnetic fluxes when the current flowing in two terminals exceeds the threshold current  $I_{TH}$ , as shown in Fig. 30(b), where the threshold current  $I_{TH}$  is adjusted by the bias current  $i_b$ , namely,  $I_{TH} = I_0 - i_b$ . In the following analyses, the current-biased Josephson junctions is represented with the symbol shown in Fig. 30(c).

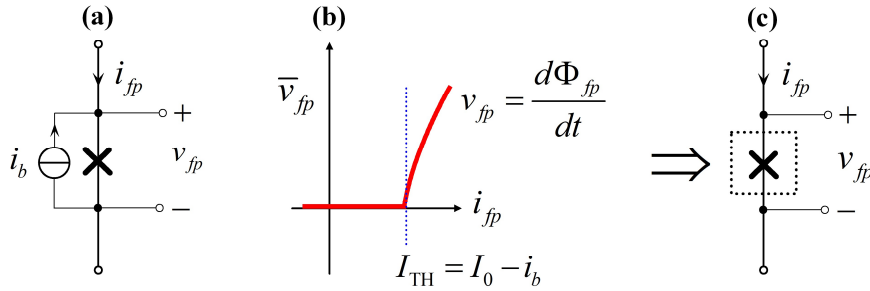


Fig. 30. Josephson junctions working as MFPs: (a) a current-biased Josephson junction; (b) the current-voltage characteristic; (c) a symbol for current-biased Josephson junctions.

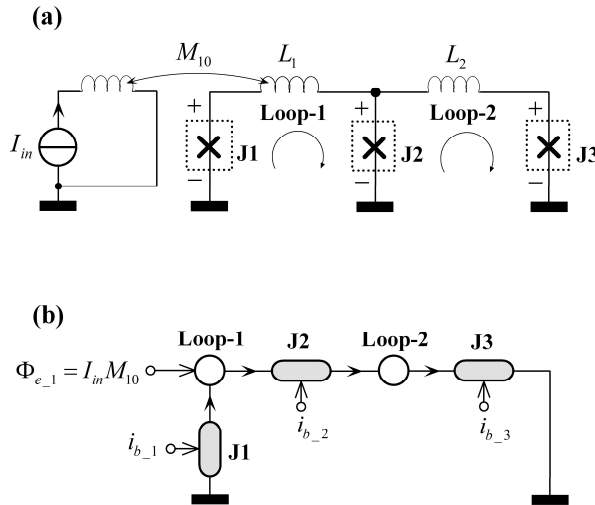


Fig. 31. (a) A Josephson-junction circuit and its (b) MFF diagram.

A typical single-flux-quantum (SFQ) digital circuit is shown in Fig. 31(a), which is a TTL-to-SFQ converter used to transform the transistor-transistor-level (TTL) clocks into SFQ signals. Its MFF diagram is shown in Fig. 31(b). The working principle of TTL-TO-SFQ is intuitively interpreted by the MFF diagram in Fig. 32.

1) As shown in Fig. 32(a), a negative  $I_{in}$  induces an external charge  $\Phi_{e-1}$  in Loop-1, and lowers the loop current in Loop-1; the low loop current will turn on the junction J1 to pump a flux-quantum to Loop-1.

2) With one flux-quantum filled in Loop-1, the loop current in Loop-1 increases and turns off the diode J1, as shown in Fig. 32(b).



3) When the current  $I_{in}$  returns to zero, the loop-current in Loop-1 will turn on J2 to transfer the flux-quantum from Loop-1 to Loop-2, as shown in Fig. 32(c).

4) The flux-quantum pumped in Loop-2 will be further be transferred by J3 to the outer-loop, as shown in Fig. 32(d).

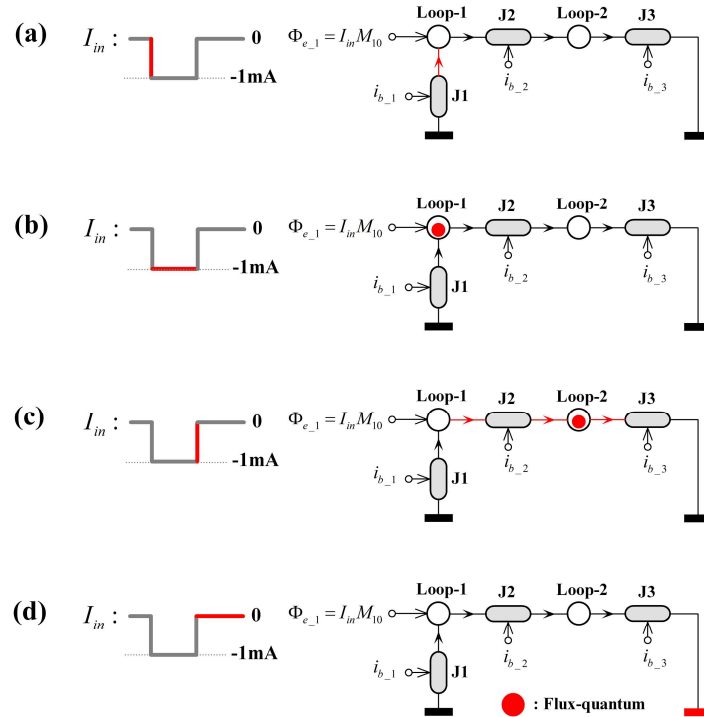


Fig. 32. Working principles of a Josephson-junction circuit depicted by MFF diagram. (a) mesh current in Loop-1 is lowered to turn J1 on, when  $I_{in}$  is lowered from 0 mA to -1mA; (b) J1 pumps one flux quantum into Loop-1; the mesh current in Loop-1 is increased to turn J1 off; (c) J2 pumps the flux quantum into Loop-2, when  $I_{in}$  returns to 0 mA; (d) J3 pumps the flux quantum to the outer-loop.

We have demonstrated the application of MFF diagrams in the design and analysis of various Josephson junction circuits such as superconducting quantum interference devices (SQUID) and SFQ circuits, more details can be find in the references [13, 14]. To be noticed that, the MFPs are called the magnetic-flux generators (MFGs) in the previous publications.

## 7. Discussion

### A. Comparison between PN-junction and Josephson junction circuits

The comparison between the PN-junction circuit and the Josephson junction circuit is depicted in Fig. 33. In the conventional circuit theory, PN junction circuits and Josephson junction circuits seem to have nothing in common:

1) **PN junctions are phase-independent devices** defined with VCRs, while **Josephson junctions are phase-dependent devices** defined with phase-current relations (PCRs). However, they are both treated as ECPs by conventional circuit theory, although they have totally different current-voltage characteristics.

2) **PN-junction and Josephson junction have totally different topologies in their application circuits**, due to their totally different VCRs. Therefore, electronics engineers will find it easy to read the PN-junction circuit shown in Fig. 33(c1), but will be confused by the Josephson junction circuit shown in Fig. 33(c2) for the questions such as, what is the physical entity of SFQ logics, and how to define the ‘0’ and ‘1’ states of SFQ logics.

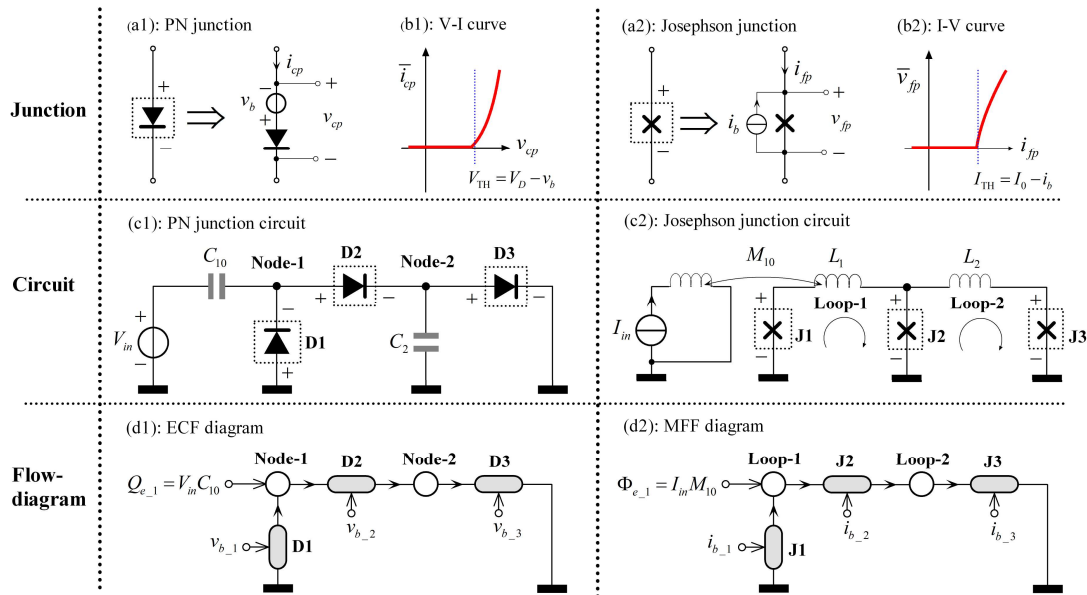


Fig. 33. Comparisons between the PN-junction and Josephson junction circuits, in junction models, circuit diagrams, and flow diagrams.

Our ECF diagram and MFF diagram visualizes the dynamics of electric circuits from the views of electric and magnetic fields. The ECF diagram shown in Fig. 33(d1) and the MFF diagram shown in Fig. 33(d2) share the same structure that reveal the **charge-flux duality** between the PN-junction circuit and the Josephson junction circuit.

1) Depicted by the ECF diagram shown in Fig. 33(d1), **PN junctions are diodes in transferring the electric charges**; the PN junction circuit is an ECP network with charges as energy carriers.

2) Depicted by the MFF diagram shown in Fig. 33(d2), **Josephson junctions are diodes in transferring magnetic fluxes**; the Josephson junction circuit is an MFP network with fluxes as the energy carriers.

### B. Duality between ECF diagram and MFF diagram

ECF and MFF diagrams exhibit the duality in the system models shown in Fig. 17 and Fig. 28. An ECF diagram is dual to an MFF diagram, if their circuit descriptions in Table 7 meet the duality principle [21]. However, the duality conditions for ECF diagram and MFF diagram cannot always be satisfied:

1) There is **an asymmetry** between  $\sigma_n$  and  $\sigma_m$ . ECPs in ECF diagrams have only two terminals, while MFPs in MFF diagrams can have more than two terminals. Therefore, there are no more than two non-zero elements in the row of  $\sigma_n$ , while there is no limitation for the row of  $\sigma_m$ . In the references [13, 14], there are a lot of MFF diagrams which MFPs have more than two terminals. Those MFF diagrams are quite different with the conventional circuit diagrams where circuit elements always have two terminals.

2) There are **asymmetries** between,  $C_n$  and  $L_m$ , and between  $C_{fp}$  and  $L_{cp}$ . It is not ensured to find an equivalent  $C_n$  for any  $L_m$ , and an equivalent  $C_{fp}$  for any  $L_{cp}$ , because the capacitances describe couplings of divergence fields, while the inductances describe the couplings of curl fields.

Table 7. Descriptions of ECF and MFF diagrams

	ECF diagram	MFF diagram
Inputs	$\mathbf{v}_b, \mathbf{Q}_e$	$\mathbf{i}_b, \Phi_e$
Outputs	$\mathbf{v}_n, \mathbf{Q}_{cp}$	$\mathbf{i}_m, \Phi_{fp}$
Connections	$\sigma_n, C_n, L_{cp}$	$\sigma_m, L_m, C_{fp}$
Devices	$F_{EIS}(\mathbf{v}_{EIS}, \mathbf{Q}_{cp}, t) = 0$	$F_{EIP}(\mathbf{i}_{EIP}, \Phi_{fp}, t) = 0$
Restriction	Every ECP has only two lines connected to ECCs	No restriction

### C. Circuit analysis using ECF and MFF diagrams

The circuit analysis methods using ECF and MFF diagrams are exhibited in Fig. 34: First, a given circuit is modeled as an ECP network or an MFP network, depending on what kind of energy carrier (charge or flux) is based.

Second, extract the circuit descriptions from the ECP network or the MFP network.

Finally, draw the ECF diagram or the MFF diagram, and set up circuit equations accordingly, for circuit simulations and optimizations.

### D. Circuit design using ECF and MFF diagrams

The circuit design methods using ECF and MFF diagrams are illustrated in Fig. 35:

First, a given circuit design specification is implemented with the ECF diagram or the MFF diagram, in the conceptual design stage, where the design scheme can be directly vilified with the simulations of system models shown in Fig. 17 and 28.

Second, export the circuit disruptions to build the ECP network or the MFP networks.

Finally, transform the ECP network or the MFP network into schematics for physical implementations.

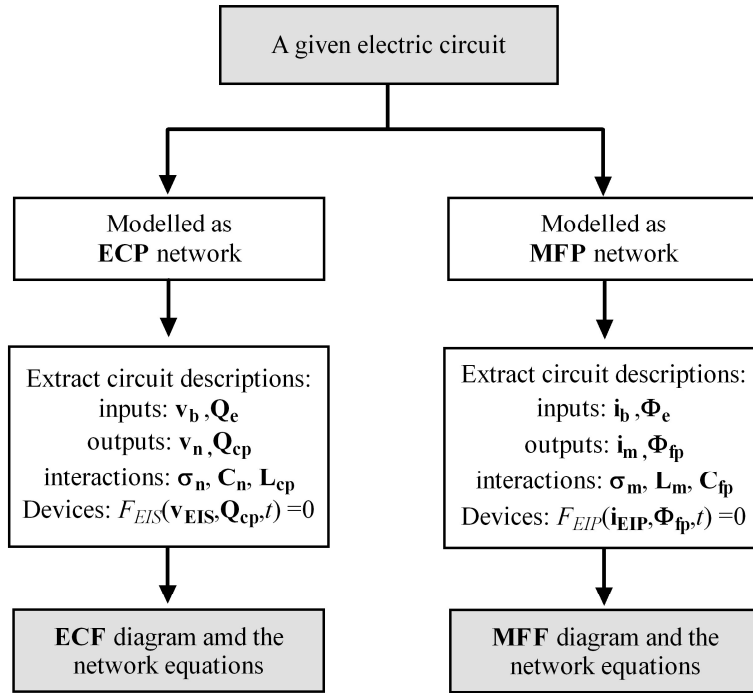


Fig. 34. Circuit analysis methods based on ECF and MFF diagrams.

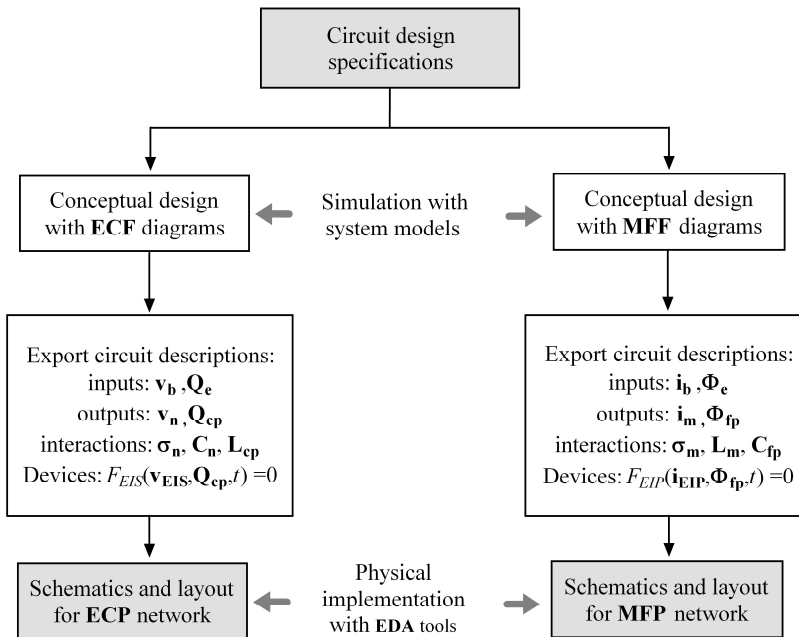


Fig. 35. Circuit design methods based on ECF and MFF diagrams.

### E. Insights to circuit design brought by ECF and MFF diagrams

Our ECF and MFF diagrams reveal the interaction mechanisms of circuit devices with electromagnetic fields, for all kinds of electric circuits:

1) **A circuit depicted by ECF diagram, looks like a kind of molecule composed of ECPs and ECCs, and the connections defined in  $\sigma_n, C_n,$  and  $L_{cp}$ , are accordingly**

the chemical bonds.

2) **A circuit depicted by MFF diagram, looks like a kind of molecule composed of MFPs and MFCs**, with the connections defined in  $\sigma_m$ ,  $L_m$ , and  $C_{fp}$ , as the chemical bonds.

With ECF and MFF diagrams, the circuit design is similar to the design of molecules, and can be also supported by the AI tools based on machine-learning [12, 35-37].

#### F. Advantages of ECF and MFF diagrams

The features and applications of three kinds of diagrams are summarized in Table 8. The advantages of ECF diagram and MFF diagram are:

1) **ECF and MFF diagrams are the interaction diagrams of circuit devices and electromagnetic fields**; they contain the complete descriptions of electric circuits, including all the electric couplings between nodes and the magnetic couplings between branches. Conventional circuit diagrams are mathematic model based on graph-theory and Kirchhoff's laws, which are the approximations of practical circuits; they are not good at modeling the mutual inductances between branches.

2) **ECF and MFF diagrams are the common physical language for both phase-independent and phase-dependent circuits**. The conventional circuit diagrams are the approximate models only suitable for phase-independent circuits.

3) **ECF and MFF diagrams are the graphical expressions of circuit equations, and can be directly calculated**. The analyses of conventional circuit diagrams require the expertise of circuit theory and the support of SPICE tools.

In summary, our ECF and MFF diagrams realize the physical descriptions of electromagnetic fields in electric circuits, and unify the design and analysis for both the phase-independent and phase-dependent circuits; they will be more precise and powerful than the conventional circuit diagrams, in developing EDA tools.

Table 8. Features of three kinds of electric circuit diagrams

	Support	Functions	Components
Schematic for implementaion	Engineers + EDA tools	To extract netlist for layout or PCB design	1) devices with terminals 2) undirected wires
Symbolic circuit diagram	Engineers + SPICE tools	To be analysed for circuit equations derivation.	1) basic circuit elements 2) undirected wires
ECF and MFF diagrams	Engineers + AI tools	Graphical expreession of circuit equations	1) two kinds of objects 2) directed wires

## 8. Conclusion

We present a general electromagnetic-field-based circuit theory to unify the design and analysis for both phase-independent and phase-dependent circuits. This theory is based on the physics of electromagnetic fields, and derives two dynamic models for electric circuits, directly from Maxwell's equations rather than the Kirchhoff's laws used in the conventional circuit theory. This theory develops ECF and MFF diagrams to visualize the interactions between circuit devices and electromagnetic fields. The ECF and MFF diagrams are the physical descriptions of electric circuits, different with the conventional circuit diagrams which are the structural models based on the graph-theory and Kirchhoff's laws. The major conclusions by this theory are follows:

1) Electric circuits with charges as the energy carriers, are modeled as ECP networks, and electric circuits with fluxes as the energy carriers are modeled as MFP networks.

2) An ECP network is composed of ECPs and ECCs, where ECPs exchange charges and energies through ECCs; its dynamics are described by the model shown in Fig. 17. An MFP network is consisted of MFPs and MFCs, where MFPs exchange fluxes and energies through MFCs; its dynamics are described by the model shown in Fig. 28.

3) ECF diagrams are the interaction diagrams of ECP networks; they are the graphical implementations of the system model of ECP networks. MFF diagrams are the interaction diagrams of MFP networks; they are the graphical expressions of the system model of MFP networks.

The ECF and MFF diagrams implement the physical descriptions for electric circuits, and make electric circuits to be designed and analyzed like the molecules composed of two kinds of atoms. They are more precise and concise to be read by artificial intelligence programs, than the conventional circuit diagrams, and therefore can be applied to develop the AI-aided EDA tools.

## Acknowledgements

## References

- [1] C. K. Alexander, M. N. Sadiku, and M. Sadiku, *Fundamentals of electric circuits*. New York, USA: McGraw-Hill 2009.
- [2] G. Kirchhoff, "On the Solution of the Equations Obtained from the Investigation of the Linear Distribution of Galvanic Currents," *IRE Transactions on Circuit Theory*, vol. 5, no. 1, pp. 4-7, 1958, doi: 10.1109/tct.1958.1086426.
- [3] Franco Maloberti and A. C. Davies, *A Short History of Circuits and Systems*. The Netherlands: River Publishers, 2016.
- [4] A. Sangiovanni-Vincentelli, "The tides of EDA," *IEEE Design & Test of Computers*, vol. 20, no. 6, pp. 59-75, 2003, doi: 10.1109/mdt.2003.1246165.
- [5] L. W. Nagel, "SPICE2 : A Computer Program to Simulate Semiconductor Circuits," Ph.D,

- Electronic Research Laboratory, College of Engineering, University of California, Berkeley, Berkeley, 1975.
- [6] S. R. Whiteley, "Josephson junctions in SPICE3," *IEEE Transactions on Magnetics*, vol. 27, no. 2, pp. 2902-2905, 1991, doi: 10.1109/20.133816.
- [7] S. V. Polonsky, V. K. Semenov, and P. N. Shevchenko, "PSCAN: personal superconductor circuit analyser," *Superconductor Science and Technology*, vol. 4, no. 11, pp. 667-670, 1991, doi: 10.1088/0953-2048/4/11/031.
- [8] M. Kiviranta, "Superconductive Circuits and the General-Purpose Electronic Simulator APLAC," *IEEE Transactions on Applied Superconductivity*, vol. 31, no. 4, pp. 1-5, 2021, doi: 10.1109/tasc.2021.3068780.
- [9] J. A. Delport, K. Jackman, P. I. Roux, and C. J. Fourie, "JoSIM—Superconductor SPICE Simulator," *IEEE Transactions on Applied Superconductivity*, vol. 29, no. 5, pp. 1-5, 2019, doi: 10.1109/tasc.2019.2897312.
- [10] M. Fayazi, Z. Colter, E. Afshari, and R. Dreslinski, "Applications of Artificial Intelligence on the Modeling and Optimization for Analog and Mixed-Signal Circuits: A Review," *IEEE Transactions on Circuits and Systems I: Regular Papers*, vol. 68, no. 6, pp. 2418-2431, 2021, doi: 10.1109/tcsi.2021.3065332.
- [11] X. Li, X. Zhang, F. Lin, and F. Blaabjerg, "Artificial-Intelligence-Based Design for Circuit Parameters of Power Converters," *IEEE Transactions on Industrial Electronics*, vol. 69, no. 11, pp. 11144-11155, 2022, doi: 10.1109/tie.2021.3088377.
- [12] E. Afacan, N. Lourenço, R. Martins, and G. Dündar, "Review: Machine learning techniques in analog/RF integrated circuit design, synthesis, layout, and test," *Integration*, vol. 77, pp. 113-130, 2021, doi: 10.1016/j.vlsi.2020.11.006.
- [13] Y. L. Wang, "Magnetic-Flux-Flow Diagrams for Design and Analysis of Josephson Junction Circuits," (in English), *Ieee Transactions on Applied Superconductivity*, vol. 33, no. 7, pp. 1-8, Oct 2023, doi: 10.1109/Tasc.2023.3290199.
- [14] Y. L. Wang, "A general flux-Based Circuit Theory for Superconducting Josephson Junction Circuits," *arXiv:2308.01693*, pp. 1-35, 2023, doi: 10.48550/ARXIV.2308.01693.
- [15] Y. S. Chauhan *et al.*, "BSIM6: Analog and RF Compact Model for Bulk MOSFET," *IEEE Transactions on Electron Devices*, vol. 61, no. 2, pp. 234-244, 2014, doi: 10.1109/ted.2013.2283084.
- [16] S. Polonsky, P. Shevchenko, A. Kirichenko, D. Zinoviev, and A. Rylyakov, "PSCAN'96: new software for simulation and optimization of complex RSFQ circuits," *IEEE Transactions on Applied Superconductivity*, vol. 7, no. 2, pp. 2685-2689, 1997, doi: 10.1109/77.621792.
- [17] H. Shichman and D. A. Hodges, "Modeling and simulation of insulated-gate field-effect transistor switching circuits," *IEEE J Solid-St Circ*, vol. 3, no. 3, pp. 285-289, 1968, doi: 10.1109/jssc.1968.1049902.
- [18] S. Franco, *Analog Circuit Design: Discrete and Integrated*. McGraw-Hill, 2015.
- [19] B. Razavi, *Design of Analog CMOS Integrated Circuits*. New York, United States of America: McGraw-Hill Education, 2017, pp. 1-44.
- [20] H. Chung-Wen, A. Ruehli, and P. Brennan, "The modified nodal approach to network analysis," *IEEE Transactions on Circuits and Systems*, vol. 22, no. 6, pp. 504-509, 1975, doi: 10.1109/tcs.1975.1084079.
- [21] Y. L. Wang, "An Electromagnetic-Flux-Distribution Model for Analyses of Superconducting

- Josephson Junction Circuits and Quantum Phase-Slip Junction Circuits," (in English), *Ieee Transactions on Applied Superconductivity*, vol. 32, no. 5, pp. 1-6, Aug 2022, doi: 10.1109/Tasc.2022.3162913.
- [22] K. K. Likharev, *Dynamics of Josephson Junctions and Circuits*. New York, USA: Gordon and Breach Science Publishers, 1986, pp. 151-293.
- [23] T. Van Duzer, C. W. Turner, D. G. McDonald, and A. F. Clark, "Principles of Superconductive Devices and Circuits," *Physics Today*, vol. 35, no. 2, pp. 80-81, 1982, doi: 10.1063/1.2914944.
- [24] P. Seidel, *Applied Superconductivity: Handbook on Devices and Applications*. Weinheim, Germany: Wiley-VCH Verlag GmbH & Co. KGaA, 2015.
- [25] B. D. Josephson, "Possible New Effects in Superconductive Tunnelling," (in English), *Physics Letters*, vol. 1, no. 7, pp. 251-253, 1962, doi: Doi 10.1016/0031-9163(62)91369-0.
- [26] K. K. Likharev and V. K. Semenov, "RSFQ logic/memory family: a new Josephson-junction technology for sub-terahertz-clock-frequency digital systems," *IEEE Transactions on Applied Superconductivity*, vol. 1, no. 1, pp. 3-28, 1991, doi: 10.1109/77.80745.
- [27] C. N. Lau, N. Markovic, M. Bockrath, A. Bezryadin, and M. Tinkham, "Quantum phase slips in superconducting nanowires," *Phys Rev Lett*, vol. 87, no. 21, p. 217003, Nov 19 2001, doi: 10.1103/PhysRevLett.87.217003.
- [28] J. E. Mooij and Y. V. Nazarov, "Superconducting nanowires as quantum phase-slip junctions," (in English), *Nat Phys*, vol. 2, no. 3, pp. 169-172, Mar 2006, doi: 10.1038/nphys234.
- [29] T. T. Hongisto and A. B. Zorin, "Single-charge transistor based on the charge-phase duality of a superconducting nanowire circuit," (in English), *Phys Rev Lett*, vol. 108, no. 9, p. 097001, Feb. 2012, doi: 10.1103/PhysRevLett.108.097001.
- [30] A. J. Kerman, "Flux-charge duality and topological quantum phase fluctuations in quasi-one-dimensional superconductors," (in English), *New J Phys*, vol. 15, no. 10, p. 105017, Oct 18 2013, doi: 10.1088/1367-2630/15/10/105017.
- [31] A. Malekpoor, S. A. Hashemi, and S. Jit, "A Direct Inverter Gate Logic Circuit Based on Quantum Phase Slip Junctions," *IEEE Transactions on Applied Superconductivity*, vol. 32, no. 8, pp. 1-8, 2022, doi: 10.1109/tasc.2022.3195786.
- [32] U. S. Goteti and M. C. Hamilton, "Charge-Based Superconducting Digital Logic Family Using Quantum Phase-Slip Junctions," *IEEE Transactions on Applied Superconductivity*, vol. 28, no. 4, pp. 1-4, 2018, doi: 10.1109/tasc.2018.2803123.
- [33] L. Schindler and C. Fourie, "Application of Phase-Based Circuit Theory to RSFQ Logic Design," (in English), *Ieee Transactions on Applied Superconductivity*, vol. 32, no. 3, pp. 1-12, Apr 2022, doi: 10.1109/Tasc.2022.3142278.
- [34] D. K. CHENG, *Field and Wave Electromagnetics 2nd edition*. INDIA: PEARSON INDIA, 2014, pp. 307-346.
- [35] V. Hamolia and V. Melnyk, "A Survey of Machine Learning Methods and Applications in Electronic Design Automation," presented at the 2021 11th International Conference on Advanced Computer Information Technologies (ACIT), Deggendorf, Germany, 15-17 September, 2021.
- [36] S. Devi, G. Tilwankar, and R. Zele, "Automated Design of Analog Circuits using Machine Learning Techniques," presented at the 2021 25th International Symposium on VLSI Design and Test (VDATE), Surat, India, 16-18 September, 2021.
- [37] Z. He *et al.*, "ChatEDA: A Large Language Model Powered Autonomous Agent for EDA,"



presented at the 2023 ACM/IEEE 5th Workshop on Machine Learning for CAD (MLCAD), Snowbird, UT, USA, 10-13 September, 2023.